TECHNICAL UNIVERSITY OF LIBEREC
Faculty of Mechanical Engineering

Experimental verification of a gas meter channel

Master Thesis

Study programme:	N2301 Mechanical Engineering
Study branch:	Machines and Equipment Design
Author:	**Livimba Samuvanga**
Thesis Supervisors:	doc. Ing. Petra Dančová, Ph.D. Department of Power Engineering Equipment

Liberec 2021

TECHNICAL UNIVERSITY OF LIBEREC
Faculty of Mechanical Engineering

Master Thesis Assignment Form

Experimental verification of a gas meter channel

Name and surname: **Livimba Samuvanga**
Identification number: S19000334
Study programme: N2301 Mechanical Engineering
Study branch: Machines and Equipment Design
Assigning department: Department of Power Engineering Equipment
Academic year: **2020/2021**

Rules for Elaboration:

The Department of Power Engineering Equipment of the TUL has a PIV system suitable for measuring 2D and 3D velocity fields in fluids. The system is based on optical (non-contact) measurement methods, therefore the velocity fields in the measured area are not affected.
The subject of the diploma thesis is the measurement of pressure loss and analysis of homogeneity of velocity fields in the inner channel of the gas meter model. The aim of the diploma thesis is to search for measuring methods suitable for measuring pressure loss and analysis of velocity fields in flow in channels, to design a measuring stand and to perform and evaluate measurements.
Principles for elaboration:
- Overview of measuring methods.
- Description of the principles of measurement by the PIV method.
- Experiment design.
- Proposal of methodology for evaluation.
- Preparation and realization of the experiment.
- Evaluation of results.

Scope of Graphic Work:
Scope of Report: cca 60 pages
Thesis Form: printed/electronic
Thesis Language: English

List of Specialised Literature:

- SCHLICHTING, Hermann a Klaus GERSTEN. *Boundary-Layer Theory*. 9th ed. 2017. Springer, 2017. ISBN 978-3-662-52917-1.
- DOEBELIN, Ernest O. *Measurement systems: application and design*. Fourth edition. New York: McGraw-Hill Publishing Company, [1990]. McGraw-Hill international editions. Mechanical engineering series. ISBN 0-07-100697-4.
- GREATED, Clive, John COSGROVE a James BUICK. *Optical Methods for Data Processing in Heat and Fluid Flow*. Bury St. Edmunds: Professional Engineering Publishing, 2002. ISBN 1-86058-281-8.

Thesis Supervisors: doc. Ing. Petra Dančová, Ph.D.
Department of Power Engineering Equipment

Date of Thesis Assignment: November 1, 2020
Date of Thesis Submission: April 30, 2022

L.S.

prof. Dr. Ing. Petr Lenfeld
Dean

doc. Ing. Petra Dančová, Ph.D.
Head of Department

Liberec November 1, 2020

Declaration

I hereby certify, I, myself, have written my master thesis as an original and primary work using the literature listed below and consulting it with my thesis supervisor and my thesis counsellor.

I acknowledge that my bachelor master thesis is fully governed by Act No. 121/2000 Coll., the Copyright Act, in particular Article 60 – School Work.

I acknowledge that the Technical University of Liberec does not infringe my copyrights by using my master thesis for internal purposes of the Technical University of Liberec.

I am aware of my obligation to inform the Technical University of Liberec on having used or granted license to use the results of my master thesis; in such a case the Technical University of Liberec may require reimbursement of the costs incurred for creating the result up to their actual amount.

At the same time, I honestly declare that the text of the printed version of my master thesis is identical with the text of the electronic version uploaded into the IS/STAG.

I acknowledge that the Technical University of Liberec will make my master thesis public in accordance with paragraph 47b of Act No. 111/1998 Coll., on Higher Education Institutions and on Amendment to Other Acts (the Higher Education Act), as amended.

I am aware of the consequences which may under the Higher Education Act result from a breach of this declaration.

June 6, 2021 Livimba Samuvanga

ACKNOWLEDGEMENT

It is with immense gratitude; I acknowledge the support of my University for providing me this great opportunity to develop in deepest manner my engineering skills while accomplishing this diploma thesis I would like to express my sincere gratitude towards everyone who extended their priceless support for this endeavour.

I would like to thank, **Doc**. **Ing. Petra Dančová, Ph.D.,** the supervisor of this diploma thesis, for her helpful approach, commitment to measure, professional advice, and critical reminders. Without her help, I might otherwise have never encountered successfully.

Furthermore, would like to thanks, **Ing. Jan Novosad,** and **Ing. Jaroslav Pulec,** for providing guidance for the thesis writing.

I would also like to express my gratitude to the Department of Power Engineering Equipment at the Technical University of Liberec for providing me the support I required, which gave me the opportunity to proceed freely with this work.

Finally, I am grateful to thank my whole family and friends for all the support, patience and encouragement throughout my studies.

This research was funded by the project No. FW02020048 of the Technology Agency of the Czech Republic (Development of compact ultrasonic gas meter with zero upstream/downstream straight pipe) and SGS 21291 (Experimental, numerical and theoretical research in fluid- and thermo-mechanics).

TABLE OF CONTENTS

LIST OF FIGURES

1. INTRODUCTION

This project deals with the measurement of pressure loss and analysis of homogeneity of velocity fields in the inner channel of the gas meter model. The aim of the diploma thesis is to search for measuring methods suitable for measuring pressure loss and analysis of velocity fields in flow channels, to design a measuring stand and to perform and evaluate measurements.

In order to design gas flow meters properly, it is necessary to establish the physical laws governing the fluid flow in the flow channel. Fluid flow in circular and non-circular pipes is commonly used in heating and cooling applications and fluid distribution networks [1]. The fluid in these applications is mostly forced to flow by a fan or pump through a flow section. Previous studies have proposed pressure drop correlations between the friction factor and Reynolds number for the central channel, which is then used to determine the pumping power requirements [2]. Also, in a typical piping system, the pressure drop value for minimum flow rate condition is greater than the pressure drop for the maximum flow conditions [2]. Typically, this happens when the fluid comes into contact with the surface of the duct. Typically, two types of pressure drop: primary losses and secondary losses. Primary losses are where some layers rub up against others – laminar flow – or friction among particles – turbulent flow. Whereas Secondary losses occur at transitions of the duct – where it narrows or expands – and in all kinds of accessories: valves, dampers, elbows, etc. [1]

Generally, pressure drops and flow measurements depend on the density of the gas, which is a function of pressure, molecular weight, and temperature. For the same mass flow rate, pressure drop increases as density decreases. Lower gas density results if pressure or molecular weight is lower or if temperature is higher [3]. The flow velocity of the fluid in a pipe basically changes from zero at the surface when we assume a no-slip condition to a maximum at the pipe centre. In fluid flow, it is convenient to work with an average velocity which remains constant in incompressible flow when the cross-sectional area of the pipe is constant. The average velocity in heating and cooling applications may change somewhat because of changes in density with temperature. But, in practice, the fluid properties at some average temperatures are evaluated and treated as constants. Additionally, the instantaneous measurement of the velocity field is of great interest to fluid mechanic research as it enables to reveal the complete topology of unsteady coherent flow structures. [3]

Accurate measurement of a gas meter has become extremely important to companies involved in its transmission and distribution over the last decade. The main reasons for this are the increasing cost of energy, the mutual desire for fair dealing between the buyer and the seller and the increasing involvement of the institutions. Furthermore, it's important to note that, metering is directly involved in determining the financial resources of gas companies and also, the measured flow values are one of the key issues to detect leaks in pipe systems. Therefore, technical factors such as pressure drop that affect the flow patterns of fluids through the meters are of great importance to the industry and should be investigated and analysed [1]. Perhaps the most widely used flow metering principle involves placing a fixed area flow restriction of some type in the pipe or duct carrying the fluid. This flow restriction causes a pressure drop which varies with the flow rate; thus, measurement of the pressure drop by means of suitable differential-pressure pickup allows flow-rate measurement.

2. LITERATURE REVIEW

A lot of research has been made in the past dealing with the flow measurement of pressure loss and analysis of homogeneity of velocity fields by optimization and proper usage of particle image velocimetry (PIV). Some of the research articles related to this Master thesis are discussed below.

B.W. van Oudheusden [4] deals with PIV-based pressure measurement. The journal contains discussion about the methods to extract pressure fields from flow velocity field data, that were typically obtained with particle image velocimetry (PIV), by combining the experimental data with the governing equations. According to the presented paper, Accuracy aspects are discussed in relation to the most dominating experimental influences, notably the accuracy of the velocity source data, the temporal and spatial resolution and the method invoked to estimate the material derivative.

B. Wieneke [5] studied the PIV uncertainty quantification and beyond. The expression of the uncertainty of vorticity, mean value, Reynolds stresses and others were derived. The paper presented that the uncertainty of the vorticity requires the knowledge of the spatial correlation between the error of x- and y-displacement, which depends upon the measurement spatial resolution. The uncertainty of statistical quantities is often dominated by the precision uncertainty (due to the finite sample size) and decreases with the square root of the effective number of independent samples. Monte Carlo simulations were conducted to assess the accuracy of the uncertainty propagation formula and showed the accuracy of the estimated uncertainty for varying testing conditions (sample size, signal under the assumption of a Gaussian velocity error distribution, variance, and error correlation). Anisotropic denoising post-processing scheme was presented which uses the uncertainties to compare

the local flow gradients in order to devise an optimal filter kernel for reducing the noise without suppressing true small-scale flow fluctuations and preserving true velocity fluctuations above the noise level.

L.M. Giovannetti, J. Banks, S.R. Turnock, S.W. Boyd [6] discussed uncertainty assessment of coupled digital image correlation and particle image velocimetry for fluid-structure interaction wind tunnel experiments. In this paper a wind tunnel-based method was used to quantify the structural behaviour, and fluid response, of a flexible aerofoil under fluid loading. The technique measured the deflection of the structure, with high-speed stereoscopic digital image correlation (DIC). The tip vortex position was measured using high resolution stereoscopic PIV. The accuracy of the two full-field optical measurement systems was quantified and the effect of optical interactions is assessed.

J. Dekowski, M. Kocik, J. Podlihski, J. Wasilewski, J. Mizeraczyk, L. Wilczyhski, J. Kanar, and J. Stasiek [6] discussed experimental investigation of the velocity field in the flow around a ship hull model using PIV. The research revealed the sensitivity and accuracy of measurements that Concerned the experiments and proved that the PIV method perfectly met the requirements specified for ship hull model testing. The flow patterns obtained also showed that the use of the PIV technique served as the valuable source for further flow analysis as well as for numerical algorithms verification.

W. Shen, F. Song, X. Hu, G. Zhu and W. Zhu [7] discussed the experimental study on flow characteristics of gas transport in micro- and nanoscale pores. The research revealed that the flux of gas flow through the nanopores is larger than the Hagen-Poiseuille (H-P) equation by more than an order of magnitude, and thus the (H-P) equation considerably underestimates gas flux. It was discovered that in nanoscale pores, Knudsen diffusion and slip flow coexist, and that their contributions to gas flux grow as the diameter shrinks. The slip flow increases with the decrease in diameter, and the slip length decreases with the increase in driving pressure. Furthermore, the observed gas flow resistance in nano pores is lower than the predicted value, and the flow resistance lowers as the diameter shrinks, which explains the flux increase and the appearance of a significant slip length at the nanoscale. These results provided insights into a better understanding of gas flow in micro- and nanoscale pores and enabled accurate predict and actively control gas slip.

T. Araki, M.S. Kim, H. Iwai, and K. Suzuki [8] investigated gaseous flow properties in microchannels experimentally. Gaseous flow frictional resistance in a trapezoidal-cross-section microchannel was shown to be lower than in a conventional-sized channel. This reduced frictional resistance in microchannel was caused by the rarefaction effect due to extremely small dimensions of flow pas-

sages and by using Maxwell's first-order slip boundary condition; they were well able to predict the mass flow rate through microchannel and the friction constant.

N. Fujisawa, K. Nakamura, F. Matsuura and Y. Sato [9] investigated experimental methods for evaluating pressure fields in a microchannel flow using μPIV measurement in conjunction with the pressure Poisson equation. The mean velocity field in microchannel junction flows with bifurcation and confluence was measured by a μPIV system, which consisted of a CCD camera and a microscope with an in-line illumination of white light from stroboscopes. By traversing the focal plane within the microscope's depth of focus, the planar velocity fields at various cross-sections of the microchannel flow were observed. By solving the pressure Poisson equation with the experimental velocity data, the pressure contour in the microchannel flow was determined. The findings revealed that the pressure field in the microchannel junction flow closely matches the pressure field in the microchannel junction flow.

R.D. Keane and R.J. Adrian studied the methods of optimization of two pulses [10], planar PIV. The paper presented discussions about the crucial parameters required for the PIV system and for the motion of fluid. According to the discussion, six important parameters are important during the performance and optimization of PIV. Particle image density, relative in-plane image displacement, relative out-of-plane image displacement, velocity gradient parameter, and ratio of mean image diameter to interrogation spot diameter are the parameters. The study was conducted about the parameters in relation with the case of autocorrelation interrogation and the dimensionless parameter was studied with the help of Monte Carlo simulation and the criteria for optimization were presented.

G.E. Elsinga, B.W. van Oudheusden and F. Scarano [11], this paper deals with experimental assessment of tomographic-PIV accuracy. Tomographic-accuracy PIV was tested experimentally using measurements of a circular cylinder wake flow at Re_D = 2700, with light sheet thicknesses of particles and seeding densities varying from 0.01 to 0.1. The precision of the 3D particle reconstruction as well as velocity measurement were both taken into account. The experimental setup consisted of four-camera imaging system with a maximum angle between viewing directions of the same line and a slit to set the light sheet thickness and to sharply define its position in depth. The accuracy of the measured velocity was assessed by a comparison with Stereo-PIV. The mean and RMS velocity were found to coincide within 0.5m/s and 0.3 m/s, respectively (corresponding to 0.30 and 0.18 voxel particle displacement). Furthermore, reconstruction noise or ghost particles were discovered to have just a minor impact on cross-correlation.

3. THEORETICAL DESCRIPTION [12]

This section delves into the theoretical explanation of fluid dynamics, which is a critical component and the foundation for experimentation. The fluid utilized in the experiment is gas.

3.1. Newtonian Fluid

When subjected to a shear stress, a fluid is described as a substance that undergoes continuous deformation. The fluid's resistance to deformation is primarily quantified in terms of the fluid property known as viscosity.

Only if the viscous forces from the flow are linearly proportional to the rate of strain is a fluid Newtonian. The viscosity tensor of a Newtonian fluid must be constant and independent of both stress and strain. While no real fluid exactly follows the Newtonian model, routinely used liquids and gases, such as water and air, are considered Newtonian. As a result, at a given temperature, Newtonian fluids have constant viscosity. The viscosity of Newtonian fluids is unaffected by the rate of change of shear stress. Air, water, glycerol, oils, a wide range of fluids, mineral oil, and gasoline are examples of Newtonian fluids. The behaviour of a Newtonian fluid is depicted in the diagram below.

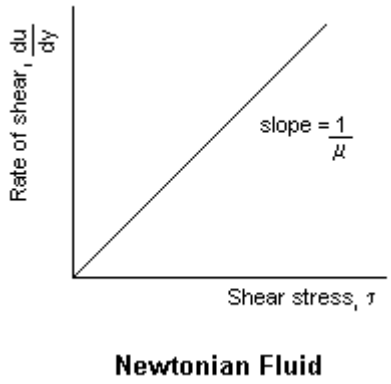

Figure 1: Behaviour of a Newtonian fluids [12]

For an incompressible Newtonian fluid, the relation can be given by the equation below as,

$$\boldsymbol{\tau = -\mu \frac{du}{dy}} \qquad (1)$$

where, τ (N) is the drag experienced in the fluid (shear stress), μ is the viscous tensor, which is the shear viscosity of the fluid and, $\frac{du}{dy}$ is the velocity component derivative relative to the displacement in perpendicular direction.

External forces generated by the surrounding fluid will affect a flowing liquid or gas element, including forces like viscous stress, which can produce flow disruptions and may be evaluated quantitatively using the above equation.

3.2. Reynolds Number

The geometry, surface roughness, flow velocity, surface temperature, and fluid type all play a role in the transition from laminar to turbulent flow. Osborne Reynolds found in the 1880s that the flow regime is mostly determined by the ratio of inertial forces to viscous forces in the fluid. [13] The viscous force will try to keep the flow motionless and stable. The inertial force, on the other hand, will try to push the fluid, causing oscillations and instability. [14] For internal flow in a circular pipe, this ratio is known as the Reynolds number.

$$\mathbf{Re} = \frac{Inertial forces}{Viscous forces} = \frac{u_{avg} D}{\vartheta} = \frac{\rho u_{avg} D}{\mu} \qquad \textbf{(2)}$$

3.3. Hagen-Poiseuille (H-P) equation

The Hagen–Poiseuille equation, or sometimes known as the Hagen–Poiseuille law, Poiseuille law or Poiseuille equation, is a physical law that gives the pressure drop in an incompressible and Newtonian fluid for a laminar flow flowing through a cylindrical pipe of constant cross section. The law shows that flow rate increases with pressure difference, and decreases with pipe length or fluid viscosity. Meaning the more pressure that is applied to the fluid at the pipe opening, the faster the fluid should flow. The longer the pipe or the stickier the fluid, the harder it is to get the fluid to flow. Its worthy noting that the result of the Hagen-Poiseuille equation is that flow rate increases with the fourth power of the radius. Therefore, pipe diameter has a big impact on how easily fluid flows down a channel. [16]

$$\Delta P = \frac{8\mu LQ}{\pi R^4} \qquad \textbf{(3)}$$

Where ΔP = pressure difference between the two ends, μ = dynamic viscosity, L = length of pipe, Q = volumetric flow rate, π = pi, and R = pipe radius.

3.4. Bernoulli's equation

Pressure, velocity, and elevation are all balanced by Bernoulli's equation. This equation explains how the speed of a fluid relates to its pressure. Places of higher fluid speed will have less pressure than points of slower fluid speed in a horizontal flow of fluid. [15]

$$p_1 + \frac{1}{2}\rho u_1^2 + \rho g h_1 = p_2 + \frac{1}{2}\rho u_2^2 + \rho g h_2 \qquad \textbf{(4)}$$

Where ρ is the fluid density, g is acceleration due to gravity, p_1 is the pressure at elevation 1, u_1 is velocity at elevation 1, h_1 is height at elevation 1, p_2 is pressure at elevation 2, u_2 is velocity at elevation 2, and h_2 is height at elevation 2

4. EXPERIMENTAL DESCRIPTION

Explanation of the process of experimentation using Particle Image Velocimetry, types and methods, their limitations, process of analysis using obtained results are explained in this section. In this Master thesis, Planar PIV is used for capturing the two-dimensional images of velocity fields with two components and then pressure based PIV is evaluated.

4.1. PRINCIPLES OF MEASUREMENT

Flow measuring methods

There are many pressures and velocity-based measurement techniques available today. An important consideration when selecting a measurement technique for an experimental or research topic is that, the best methodology largely depends on the specific problem being addressed. Below is a description of just a few.

Pressure measurements are frequently recovered pointwise, such example with pressure taps or Pitot tubes. It takes time, effort, and money to instrument wind tunnel models using pressure sensors [17]. For example, single-point measurement techniques, such as Laser Doppler Velocimetry (LDV) or Hot Wire Anemometry (HWA), are usually the proper choice when flow statistics need to be accurately determined. On the other hand, a "multi-point" technique, such as Particle Image Velocimetry (PIV), is necessary for the measurement of instantaneous distribution of vorticity, in order to capture the dynamics of eddy structures in turbulent flows. However, when limited optical access makes the use of PIV impractical or laborious (e.g., propeller inter-blade flow, rudder-propeller interaction), LDV may be better suited to measure steady and periodic flows. The velocity dynamic range, spatial resolution, and frequency responsiveness, as well as more practical factors like the volume of data to be managed, facility occupancy, and processing time, all influence the methodology choice for a given application [18]. The experimentalist or researcher should carefully consider the pros and cons of each measurement technique, both from the point of view of its ability to analyse the phenomenon and measure the flow quantities of interest and from the point of view of the overall complexity and cost of implementation. Often, the result of this

analysis is a trade-off between conflicting requirements and constraints, which might involve both technical and practical issues.

1. Flow visualisation technique: it is based on one of two basic principles, the introduction of tracer particles or the detection of flow related changes in fluid optical properties. In gas flows, smoke, helium-filled “soap” bubbles, or gas molecules made luminous by ionizing electric spark have served as tracers. Shadowgraph, schlieren, and interferometer techniques [1] employ, in different ways, the variation in refractive index of the flowing gas density. For compressible flows (Mach number above 0.3), density varies with velocity sufficiently to produce measurable effects. More recently, the optical pressure-sensitive technique, known as pressure-sensitive paint (PSP) has been developed, which relies on the application of a pressure-sensitive luminescent. [19] [20]

2. For velocity field measurements relating to fluid flows, PIV is now regarded as a key experimental technique. The technique helps to produce quantitative visualizations pertaining to the instantaneous flow patterns, which are usually employed for supporting the validation of numerical simulations or the development of phenomenological models pertaining to complex flows.

Therefore, it is the aim of this research to come up with suitable methods for; measuring pressure loss, analysis of velocity fields in flow in channels using the Particle Image Velocimetry (PIV) technique and to thereafter, design an evaluable measuring stand.

4.1.1. Particle Image Velocimetry (PIV) method

Particle image velocimetry (PIV) is an optical non-invasive technique method of flow visualization used in modern experimental fluid mechanics and research, that utilizes a predefined laser plane to illuminate tiny particles dispersed throughout the fluid in quick succession. PIV is mainly used to obtain instantaneous velocity measurements and other properties in fluids. The difference in particle location between successive photographs can be used to estimate the velocity of each particle in the photos, and hence the flow field over the entire imaging area. [21] PIV setup consists of a high-speed camera, a high-power multi-pulsed laser, an optical arrangement to convert laser output light to a light sheet, and a synchronizer that controls the synchronization between the laser and the camera, as well as seeding particles that are added to the flow and the operating flow channel. [6] A PIV software is used to post process the recorded images, dividing with the known time between the two images captured, the displacement vectors are converted into a map of so-called raw velocity vectors. For faster calculation of correlations, FFT-processing is used. PIV is based on the Eulerian method for measuring the velocity fields. This technique has the advantage of providing measurement over a large area in a short period of time.

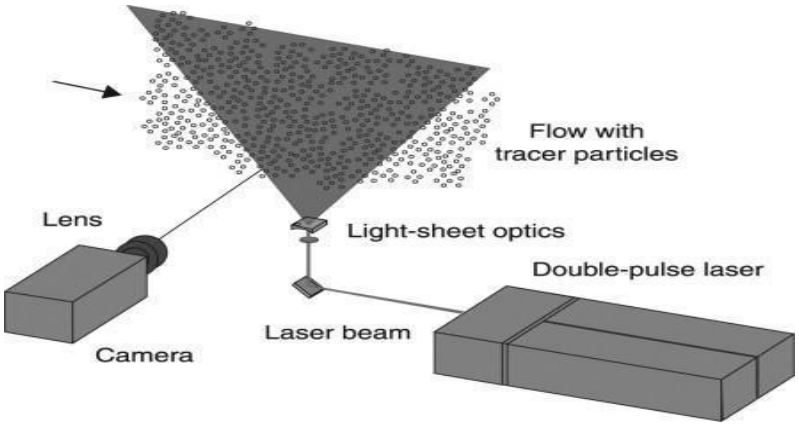

Figure 2: A typical PIV measurement set-up.

4.3. METHODS OF PARTICLE IMAGE VELOCIMETRY

The type of PIV varies depending upon the number of cameras and the kind of data measured during the experiment. Below is description of the types of PIV;

4.3.1. PLANAR PIV

The classical Planar PIV technique can be defined as a two-dimensional (2D) measuring technique and can only measure two components in the plane of the illuminating laser sheet pertaining to flow velocity vectors. Due to the perspective transformation, velocity vectors' out of-plane component gets lost, while an unrecoverable error impacts the in-plane components. [20] Since single camera is used, the calibration of the plane can be done easily and less time consuming compared to stereoscopic and tomographic PIV. An optic fibre cable or a liquid light guide connects the laser to the lens system. The experimental setup of planar PIV consists of a single camera, laser optics, host computer, synchronizer and the test channel with the fluid and tracer particles. The fluid and tracer particles are poured into the test channel. The laser light sheet is made to align with the field of view, so as to illuminate the particles to get a better visualization. The camera is then focussed on to the field of view, with the calibration done. The experimental setup is completed and the system is ready to capture the images. Depending on who is conducting the research, images are acquired with various ranges. Depending on the needs, these images are then post processed to provide relative velocity fields, pressure, and vorticity.

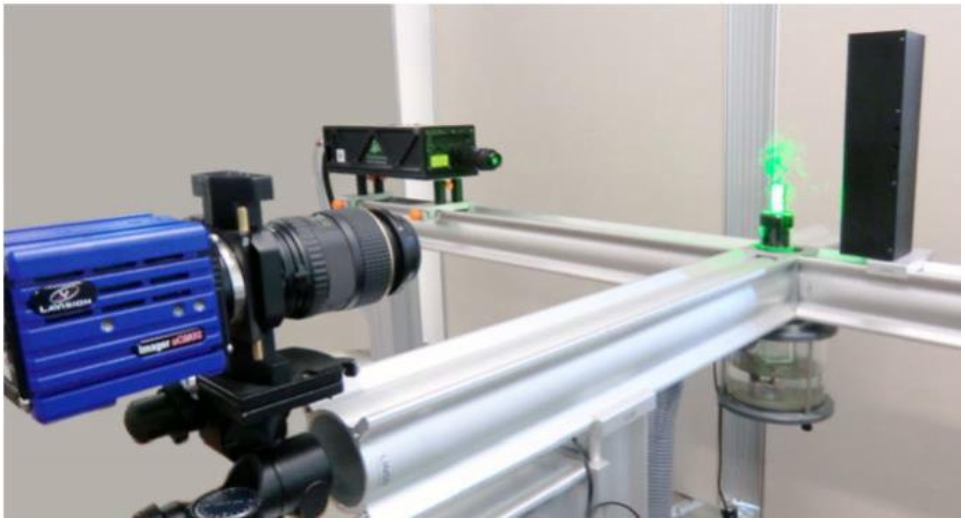

Figure 3:Experimental Setup of Planar Particle Image Velocimetry [22]

4.3.2. STEREOSCOPIC PIV

The stereo PIV technique is recognized as the easiest and most easy approach for simultaneously measuring all three components pertaining to velocity vectors in the laser illuminating plane. It uses two cameras at varied view axes or considers an offset distance to provide stereoscopic image recording (as illustrated in **Figure 4**). Reconstruction of all three components linked to the velocity vectors in the measurement plane is possible by matching the respective picture segments pertaining to the two cameras' image planes. Stereo PIV measurements have a substantially higher in-plane spatial resolution than tomographic PIV and 3D-PTV observations. With respect to the measuring plane, thousands of flow velocity vectors can be provided. [23]

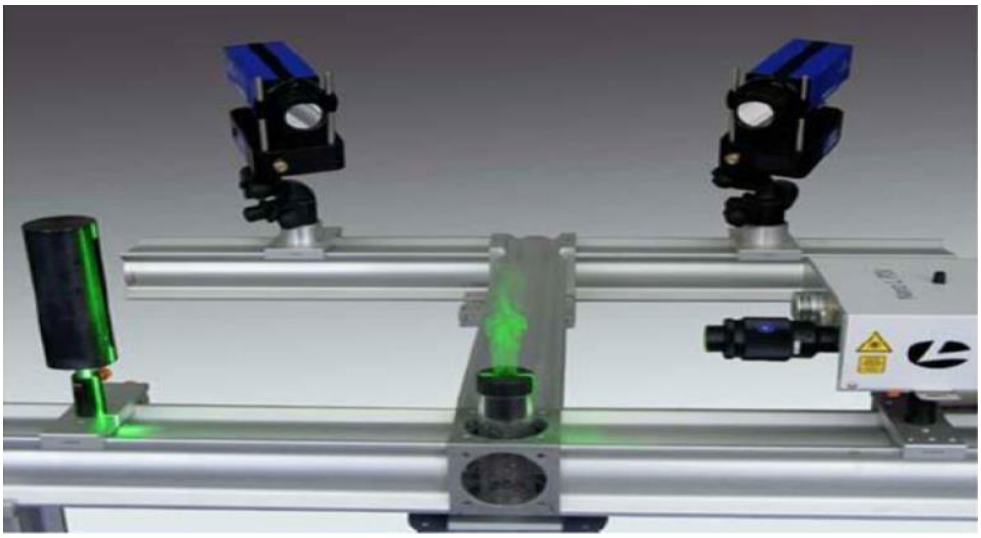

Figure 4: Stereoscopic PIV based on the principle of stereoscopic imaging [22]

4.3.3. HOLOGRAPHIC PIV

Holographic PIV [24] (as shown in Figure 1.4) employs holography techniques to record image, which allows determining all three components associated with velocity vectors for the entire volume of fluid flow. Amongst the current PIV techniques, HPIV gives the highest measurement precision as well as spatial resolution [25]. However, HPIV is also regarded as being one of the most complex PIV techniques, which needs considerable investment for optical alignments and equipment as well as requires developing advanced data processing techniques. Much effort is still needed to practically apply HPIV as a PIV technique for different complex engineering applications.

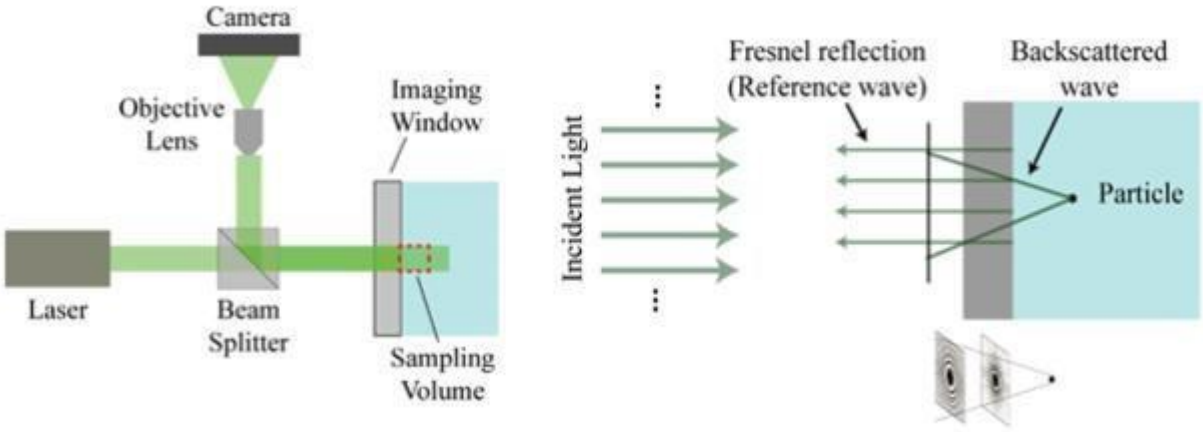

Figure 5: Experimental setup of HPIV

4.3.4. TOMOGRAPHIC PIV

TOMO PIV (tomographic particle image velocimetry) is a three-dimensional, three-component (3D3C) velocimetry technique. With the help of this method, illumination of a tracer-particle field is achieved volumetrically, which is also concurrently images from different viewing angles, while inferring of the 3D Mie-scattering field is done through tomographic reconstruction based on the simultaneous particle images which is performed with the MART algorithm, yielding a 3D array of light intensity discretized over voxels. The subsequent tomogram pairs are split into interrogation boxes (IBs), and the average particle displacement is projected through cross-correlation. Thus, T-PIV renders rapid 3D3C measurements of the fluid velocity field.

The feasibility and promise of the proposed system with four cameras are demonstrated in a computer simulated experiment of a 3D particle motion field depicting a vortex ring as illustrated in **Figure 6**.

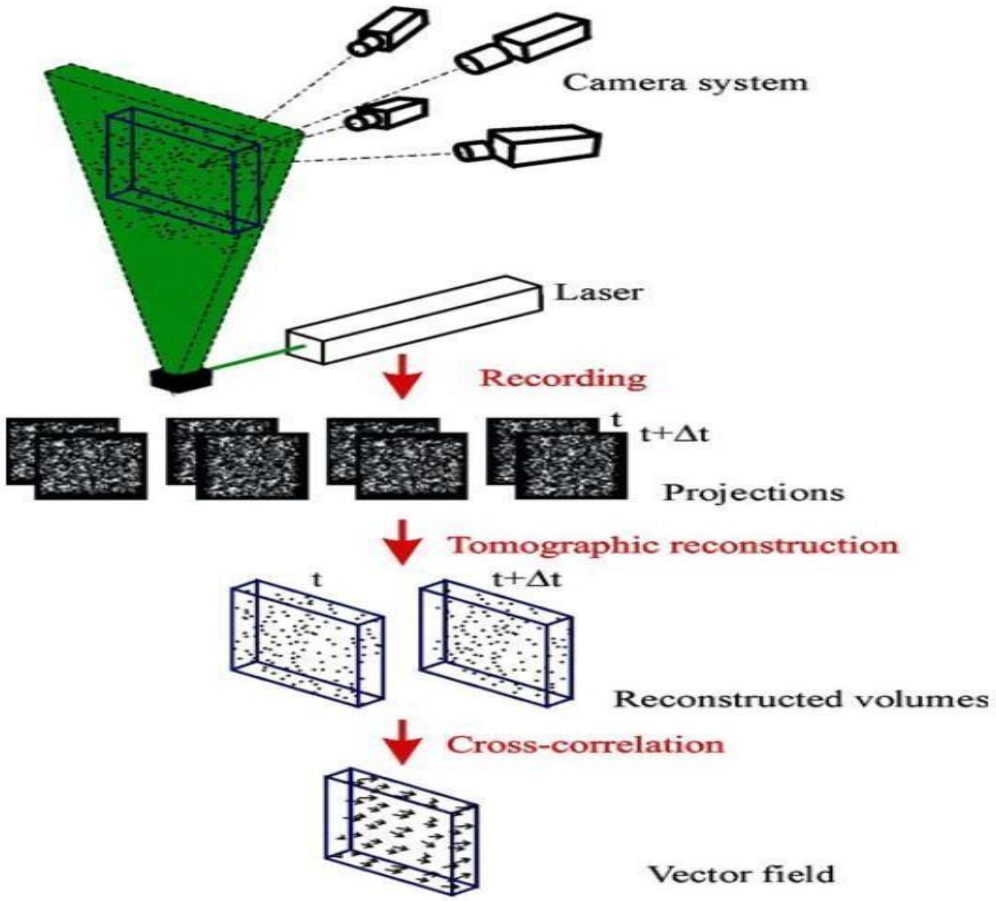

Figure 6: Principle of tomographic-PIV [26]

4.3.5. MICRO PIV

Micro PIV is flow measurements related to microfluidic devices which have been restricted to the flow's bulk characteristics, like bulk velocity, wall pressure and specific impulse (for micro-nozzles). Critical parameters to be considered during and before experimentation are the selection of cameras, optics, laser and seeding particles. It can present two dimensional two components' systems like the planar PIV and two-dimensional three component systems like the stereoscopic PIV. PIV methods are preferred for nano-scale and micro-scale fluid mechanics as these allow avoiding Brownian motion along with high seeding density.

Figure 7: Micro PIV setup [22]

4.4. BASIC ELEMENTS IN PIV TECHNIQUE

The basic elements which should be considered in implementing the PIV technique are as follows

4.4.1. Seeding

The correct choice of seeding particles is critical to the successful execution of PIV. Seed particles should be small enough to follow the flow being measured, but large enough to generate a strong scattering signal or to allow reflecting each of the measured velocity vectors. Other factors to consider are, particle size, density, shape, composition, and concentration are important factors when selecting seed particles.

The handling of commonly employed particles is not easy since most of the liquid droplets get evaporated quickly. Dispersion of solid particles is difficult since these are likely to get agglomerated. The particles need to be frequently flow introduced once prior to the entry of the gas region into the division test. The introduction process needs to be executed without disturbing the flow, for most of the current disturbance relating to numerous experiments research is not strong enough to adequately blind the particles with the liquid, therefore, particles need to be introduced through some openings. Tracer introducer such as rakes that have many small pipes with many little holes, are frequently used. Thus, there is a need for particles that could be easily transported inside small pipes

The ability of a particle to follow fluctuations in the flow depends on the particle's aerodynamic diameter (d_a) which, in turn, depends on the particle's geometric diameter (d_g) and density (ρ) according to the following equation:

$$\mathbf{d_a = d_g \sqrt{\rho}} \qquad \mathbf{(5)}$$

When d_a (aerodynamic diameter) is smaller, it has a higher frequency response and is better able to follow rapid flow fluctuations.

To have a Maximum number of PIV vectors or LDV data rates, its required to have a highest scattered light intensity from seed particles. This can be achieved by optimizing the particle surface properties and relative refractive index. Basically, a greater relative index of refraction and larger geometric particle size both help improve signal strength. i.e., the refractive index of water is considerably larger than that of air. Particle scattering in air is at least one order of magnitude more effective than in water for particles of the same size.

4.4.2. Imaging

There are two types of PIV recording modes: (1) methods that capture the illuminated flow onto a single frame, and (2) methods that produce a single illuminated image for each illumination pulse. These branches are referred to as single frame/multi-exposure PIV (put a figure for illustration) and multi-frame/single exposure PIV (put a figure for illustration), respectively. [19] The principal distinction between the two categories is that the former method, without additional effort, does not retain information on the temporal order of the illumination pulse the reconstructed displacement vector now has a directional ambiguity. This requires the development of a number of strategies to account for the directional ambiguity, including displacement biasing and so-called image shifting (i.e., using a rotating mirror or birefringent crystal), pulse tagging or colour coding 1. Multi-frame/single exposure PIV recording, on the other hand, is the method of choice if the technological conditions can be accomplished because it intrinsically retains the temporal order of the particle images. Also, in terms of evaluation, this method is far more straightforward.

Light scattering particles are introduced to the flow via Particle Image Velocimetry (PIV). With a small time, interval t, a laser beam is shaped into a light sheet that illuminates seeding particles twice. Two consecutive frames of a high-resolution digital camera are used to record the scattered light in 2D-PIV. Stereo-PIV uses two cameras with different observation angles to measure the flow velocity in the light sheet's third (out-of-plane) component.

Each camera's particle picture is segmented into small interrogation windows for velocity calculation. Cross-correlation is used to determine the average particle displacement inside an interrogation

window, followed by the localization of the correlation peak. The velocity components are calculated using the known time difference t and the measured displacement in each direction. Self-Calibration processes handle perspective correction, distortion compensation, and image mapping of the two viewpoints. Higher accuracy and spatial resolution are achieved using advanced multi-pass picture deformation algorithms.

4.5. UNCERTAINTY OF PIV TECHNIQUES

Methods and techniques used in PIV, some systematic errors may occur and should be considered when working with PIV systems. PIV limitations depend on size of the particle, velocity of the flow, and saturation of the seeding particles.

4.5.1. Dynamic range

Performance of PIV can be valued by the measurement of parameters such as Velocity dynamic range and spatial resolution. Dynamic range describes the kinematic flow properties which covers the basic of fluid dynamics. Absolute dynamic range is defined as the relative difference between maximum and minimum measurable range in the interrogation area. Since the flow can take place in both directions, the motion of minimum velocity means the minimum speed in opposite direction to maximum velocity.

Challenges to overcome during the measurement of velocity dynamic range, [27]

1. Velocity dynamic range is restricted due to the loss pairs caused by the issue between interrogation window size and in-plane displacement.
2. Underestimation of velocity gradients occurs due to the finite interrogation window because of the dependence between accuracy and spatial resolution
3. Peak locking occurs when the particle image sizes are smaller than two pixels or having poor spatial resolution. The phenomena of having discrete displacement values due to the dependence of displacement estimation on the peak interpolation function are called peak locking.

4.5.2. Lost pairs

Lost pairs are the critical errors in PIV, which are caused when the particle leaves an interrogation area or enters an interrogation area between consecutive light pulses. Because of this lost pair, there is a chance of lonely particle in the second image, which can cause error during average velocity measurement. When dealing with turbulent flow or with high velocity, there are higher chances of the particle leaving the interrogation area, which causes the velocities with small gradients to have a

greater influence during averaging calculation. This type of gradient error is known as error of velocity taking down to zero.

4.5.3. image saturation

Saturation can be poor, medium and strong. Recommended value of saturation particle is 5 per interrogation area for cross correlation and 10 particles per interrogation area for autocorrelation.

4.5.3.1.Poor saturation

The efficiency of this saturation is effective if the evaluation range is not more than a single part. The determination of average displacement is simpler, but in reality, it becomes unsuitable because of the uneven spreading of the particles, where some particles are clouded in particular evaluation and missing of particles in other. Therefore, the information obtained from the images will be incomplete.

4.5.3.2.Medium saturation

Sufficient particles are spread along the evaluation area, so that each evaluation area gets the required number of particles. In such case, the information on the velocity field can be easily achieved without any difficulties because of the complete information. The average displacement of all particles is determined by the use of an algorithm. This type of saturation is widely used by the researchers.

4.5.3.3.Strong saturation

When you have a higher saturation, it is not possible to distinguish between individual particles, and every evaluation area becomes clouded. The image of average displacement shows a cluster of particles in the flow field. Because of this, the problem of insufficient lighting may occur.

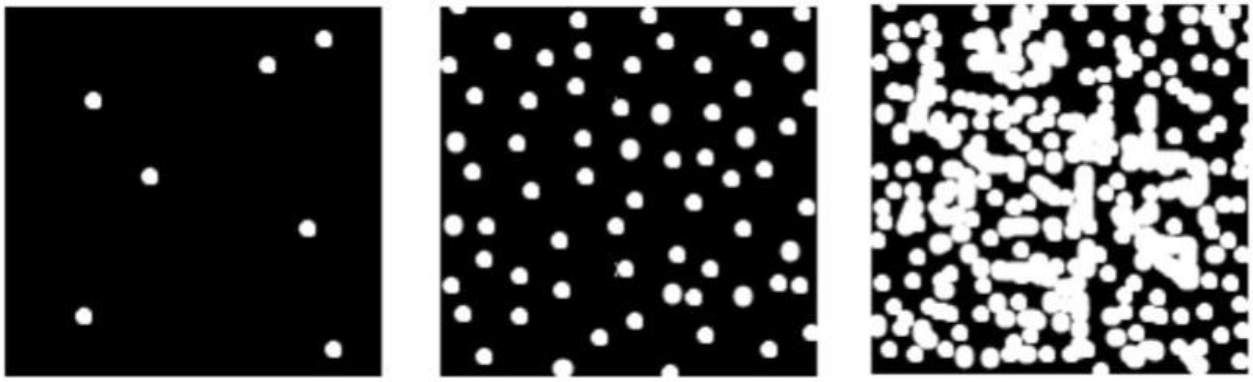

Figure 8: a. Poor saturation; b. medium saturation; c. Strong saturation [28]

4.6. MEASUREMENT ACCURACY

Main limitation for measuring accuracy includes pick-up technique, lasers and the equipment used for analysing. To get a better result from the experimentation, it is necessary to choose the reliable

size of interrogation areas. Measurement accuracy, which means increasing the spatial resolution, this can be attained by increasing the vectors needed in a single interrogation area. For eliminating the errors by lost pairs, it is suggested to choose interrogation areas which are considerably large. Further errors can be restricted by the use of certain techniques like overlap, window function, off-set, filters, etc. These applications cannot present any new information to the calculated results, but eliminating the errors for a better visualization.

4.7. POST-PROCESSING OF PIV DATA

After the images are captured by the cameras, it will be stored in the host computer using software, which is to be further processed to obtain the results. Post-processing of PIV generally includes following five steps.

4.7.1. Validation of raw data

Once the images are captured and stored, it can be able to view the raw data to check for errors. Raw data usually contains certain amount of uncertain velocity gradients that can be detected from naked eye. Because it is a time-consuming process, some kind of algorithm have to be developed, to be able to do it automatically. Validation of the raw data can be important because of the ability to remove certain images which can be identified as defects and will remove the error of handling improper information.

4.7.2. Replacement of improper data

PIV post-processing techniques require thorough information data fields to process the images to vectors. Such techniques cannot identify the vectors in the area of data drop-out, and leaves empty spaces in the result. Improvements can be made to create an algorithm for limiting this error.

4.7.3. Data reduction

Processed data are either reduced or grouped into pairs for analysis, since the algorithm cannot handle all the vectors altogether. Some of them include averaging, conditional sampling, and vector field operators.

4.8. ANALYSIS

Critical part of PIV post-processing is so much concentrated on analysis, as this can depend on the usage of the user to obtain the results. PIV is the first technique to deliver data about instantaneous velocity fields. And ever since, it has been an area of research in the field of fluid dynamics. Some of the analysis techniques include proper orthogonal decomposition and neural networking.

4.9. PRESENTATION OF THE INFORMATION

Wide ranges of software have been used for the purpose of presenting the PIV data. It can be presented in a varied form such as contour plotting, colour mapping, vector and scalar fields, graphical representation of numerical values. It is helpful for the PIV user to achieve and compare the results. It is even helpful in three-dimensional PIV data, which is difficult to analyse by any other method.

4.10. APPLICATIONS OF PIV

The application of PIV ranges from micrometres to meters depending on the phenomena, research purposes alone cover 70%, medical industries, automotive, chemical, and aerospace covers 30%. Some application includes but not limited to;

1. One can observe the flow inside blood vessels as well as the flow in rivers, ocean currents and cloud fields.
2. Biomedical researches wind tunnel, towing tanks for water flow visualization, flame visualization, and nozzles, etc.

5. EXPERIMENTAL SETUP

The experimental setup in this Master thesis for visualization of flow of the fluid using (PIV) Particle Image Velocimetry was done in several stages,

- Channel arrangement
- Seeding the particle tracers
- Illumination system
- Camera for capturing the images
- Host computer for post processing

5.1. CHANNEL ARRANGEMENT

For the purpose of this master thesis, the test section used is a transparent cylindrical pipe cross section DN80, which is parallelepiped by joining with four elbow joints with special adhesives and fasteners. The Channel is fitted with pipes (1meter each) on both sides from entry and exit for the fluid to flow along the channel. A vacuum cleaner was used to initiate the fluid flow in the channel, it was connected from exist point with a flow control meter to control the air flow and then seeding particles were introduced in the channel from entry side and sucked by the vacuum cleaner and

therefore, the flow was said to be in suction regime. The temperature of air during the experiment was found to be around 26 degrees Celsius. Below is the image of the experimental setup.

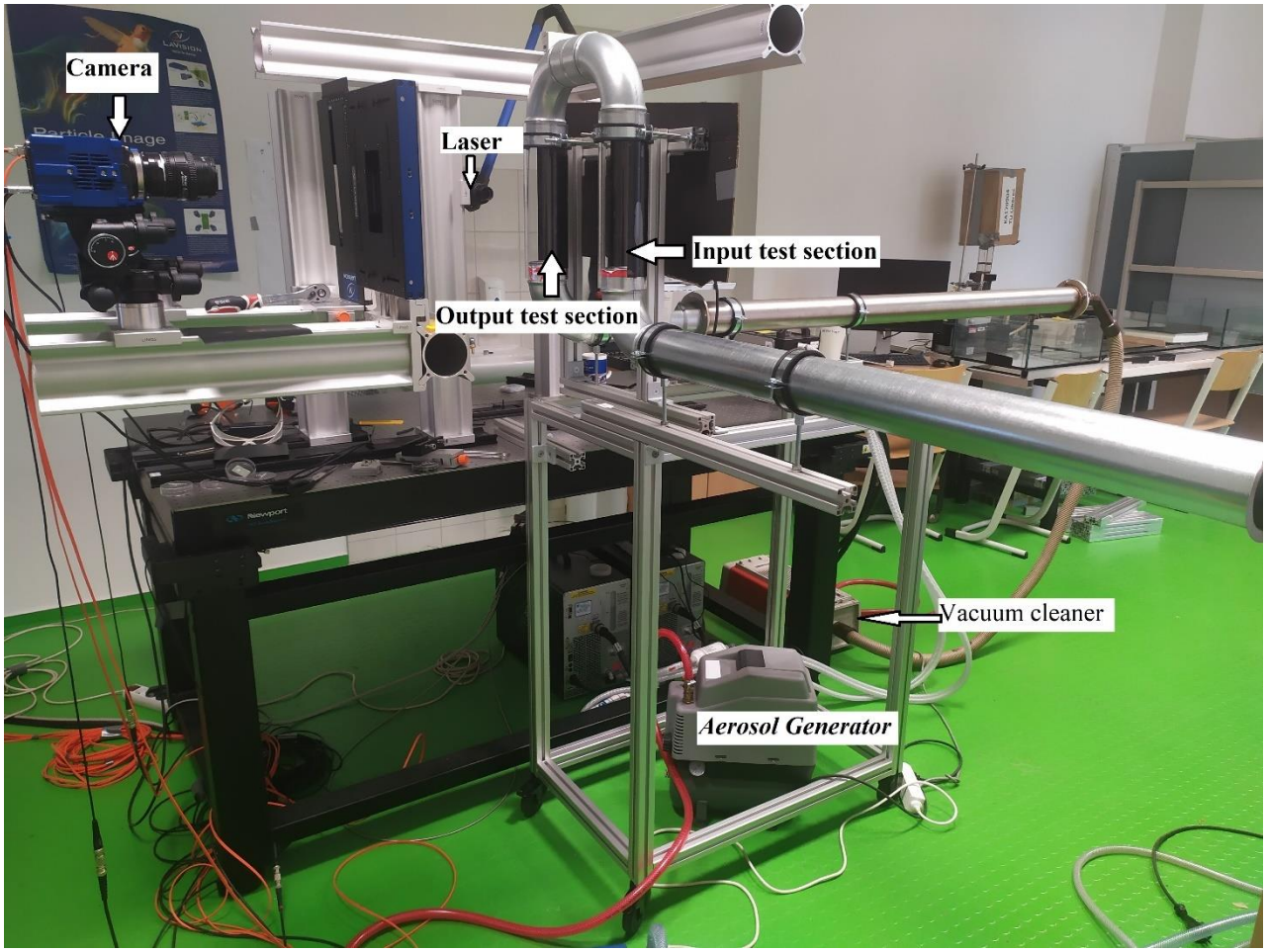

Figure 9: Experimental setup

5.2. PARTICLE TRACERS

Generally, for a gaseous flow, both liquid and solid particles can be used as tracers. For the purpose of this thesis, the LaVision Aerosol Generator which generates a polydisperse aerosol by atomizing liquids into particles in the submicrometer range was used, which sustained a counter pressure of up to 10 bar.

Figure 10: Aerosol Generator [22]

5.3. ILLUMINATION SYSTEM

Illumination system used for the purpose of this thesis was composed of light source (laser) and optics. Lasers like Argon-ion laser and Nd:Yag laser are mostly used for the illumination purpose in PIV to emit monochromatic light with high energy density which can be made into a light sheet for illuminating the tracer particles inside the test channel. This sheet of light can be achieved by a set of spherical lenses and a cylindrical lens which is made to incident on the area to be interrogated. The cylindrical lens expands the laser light into a plane, whereas the spherical lens converts the plane into a thin sheet. This laser sheet is incident on the area with a centimetre before the cylinder test section pipe (at the outlet) and 30-50 centimetres after the cylinder pipe test section (at the inlet) for visualization process. During the adjustment of light sheet, the lens of the camera should be covered with their caps in order to avoid the damage of the camera. Light sheet is adjusted manually to be in a straight line with the field of view, during calibration and during experimentation. It is done by using a detector or viewing card to bring it to the lowest possible thickness. Laser used in this experiment is double-pulsed Nd:Yag laser.

5.4. CAMERA FOR CAPTURING IMAGES

sCMOS (scientific Complementary metal-oxide-semiconductor) LaVision camera was used in this process of planar PIV. sCMOS cameras are used for its high noise immunity and relatively low static power consumption. As this is a planar PIV, one camera is used to visualize the flow of gas in the channel to measure the 2 dimensional 2 components of velocity vector. The camera can be used to capture two frames at high speed within few hundred nanoseconds as mentioned in the Table 1 below. Because of the capturing of two frames, the system uses cross-correlation analysis for processing of the images. Specific lenses have been used to capture the images like cylindrical lens, lens with band pass filter. The camera and the lasers have been mounted using rails and mounting parts, and a sliding three axis gear head. The focussing of the camera to the field of view is done by viewing the image at the computer and adjusting the aperture and the focus on the camera. A calibration sheet is used to calibrate the PIV prior to the measurements. The light sheet is aligned with the calibration sheet which is kept in the same position as the field of view. The calibration sheet consists of white dots in a black background in a perfectly machined surface for a better visualization purpose.

5.5. HOST COMPUTER

The computer system from LaVision uses dual quad-core 64bit processing unit. It contains the LaVision's internal Programmable Timing Unit (PTU), a synchronizer from LaVision, which is used to trigger the laser and camera from the computer, which is operating the hardware using the software. The photos acquired from the experiment are captured, stored, and processed using DaVis FlowMaster 10.0.4 software.

6. EXPERIMENT METHODOLOGY

The experiment was conducted after the channel was checked for leakages; laser light aligned to the field flow, and the calibration have been done. Visualization of flow in the channel was recorded for five different flow rates. The flow was recorded with the highest flow rate of 69 metres cubic per hour and lowest flow rate of 4 metres cubic per hour. 300 images were captured for each cylinder for all five flow rates. The images were combined using cross correlation and post processed.

Table 1: Variants of flowrates used for the experiment. Shows the variants of flowrates used for the experiment.

Flow rate used: 69 m^3/h

Volumetric flow rate: 0.019 m^3/s

Cross sectional area of the test section: 0.0050207 m^2

Velocity of the flow = $\frac{\text{Volumetric flow rate}}{\text{Cross section Area}} = \frac{0.019}{0.0050207} = 3.8$ m/s

Table 1: Variants of flowrates used for the experiment.

VARIANT	V01	V02	V03	V04	V05
FLOWRATE (m^3/h)	69	34	26	8	4
FLOWRATE (m^3/s)	0.019166667	0.009444444	0.007222222	0.002222222	0.001111111

MEAN VELOCITY (m/s)	3.817528764	1.88110113	1.4384891	0.442612031	0.221306015

Pressure characteristics of the elbow used for connecting the two test sections is between (10 -12 Pa) for the velocity of 3.8 m/s as seen in the **Figure 13** below,

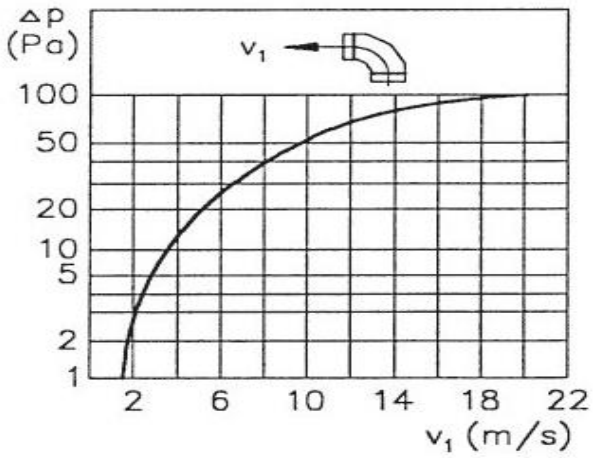

Figure 11: Pressure characteristics of the elbow used [29]

6.1. ROLE OF PRESSURE FROM PIV

For the purpose of this thesis, pressure base PIV was used during the experiment. Pressure from PIV reconstructs pressure fields from velocity fields in case of incompressible flow and the resulting pressure fields connote dynamic aspects of fluid flow in addition to kinematic aspects of velocity fields. As a well-known method reviewed by Van Oudheusden, pressure field evaluation from PIV data requires two sequential steps: pressure gradient computation from velocity field and its spatial integration by means of Poisson equation [4].

6.2. ADVANTAGES OF PRESSURE BASED PIV

There are few good, unique and important features of Pressure from PIV.

• It only takes minimum effort to define boundary condition.

• In pressure from PIV Temporal continuity of pressure is inherently enforced by the new algorithm. This reliably prevents unphysical fluctuation in the computed pressure fields, often visible for less sophisticated single time-step methods

• Pressure from PIV is able to consider an irregular measurement domain, the shape of the domain may even change in time, which are often caused by illumination limitations or image masking, for

example due to reflections or obstacles in the flow. Note that only the largest cluster of grid points, connected to each other, is regarded as a computational domain.

6.3. LIMITATION AND RESTRICTION OF PRESSURE-BASED PIV

In order to utilize Pressure from PIV appropriately, Caution was taken with regard to the following features.

• Out-of-plane motion: In 2D-PIV and Stereo-PIV systems, a spatial derivative of the third velocity component cannot be considered. Therefore, pressure results are not reliable when a large out-of-plane motion exists.

• Spatial and temporal resolution: The pressure gradient is internally calculated from discretized velocity data, which is discretized not only in space (by a grid spacing $\Delta x = \Delta y = \Delta z$) but also discretized in time by the time interval between acquisitions (Δt) for the instantaneous pressure operation. Therefore, smaller structures than the grid size and higher frequency characteristics cannot be recognized. Note that the observable minimum size and maximum frequency of flow structures follow the Nyquist limit.

• Time-averaged pressure: Fully-converged Reynolds stress fields are required for the RANS equation to determine accurate average pressure. Typically, it can be achieved by averaging a large number of velocity fields, but the required number depends on a flow characteristic. In a practical viewpoint, Reynolds's stress fields can be assumed to be fully-converged, if two average fields, which are obtained from the first half and the second half of the entire data set respectively, are nearly identical or at least very similar.

• Instantaneous pressure operation requires time-resolved data. Do not apply the operation to velocity fields that are not continuous in time (e.g., from low repetition rate double pulse recordings).

• Instantaneous pressure: It is recommended that the maximum displacement should be smaller than the final window size. The motion of fluid parcel can be assumed to be on an artificial trajectory. At the neighbouring time steps, i.e. $-\Delta t$ and $+\Delta t$ from the reference time step, the fluid parcels along the trajectory should stay within a reasonable range in order not to lose consistency.

6.4. SEQUENCE OF OPERATION

Pressure from PIV is integrated as a group of processing operations in DaVis 10. To perform a Pressure from PIV analysis, the following sequences were performed

1. Selected a velocity set as an input and add a processing operation, by selecting the processing group pressure from PIV, an entry in Operation list.
2. Set air as a working fluid where the solver recognises density and dynamic viscosity which are computed based on a specified Temperature under the standard state
3. Set solver options: Selected the time-averaged pressure processing option for the purpose of this thesis.
4. Set a boundary condition: As described earlier, a pressure field is reconstructed by solving a Poisson equation which spatially integrates a pressure gradient field. It means that at least one reference pressure value must be specified prior to solving the Poisson equation. Pressure from PIV deals with the reference pressure in terms of a boundary condition. Pressure from PIV has three boundary condition options: (a) specify an average pressure, (b) Bernoulli's principle, and (c) specify pressures at points. For the purpose of this thesis option (b) Bernoulli's principle was used as it gave more realistic solutions. This option requires free-stream velocity and pressure values and a sampling region. Entire pressure values are uniformly adjusted to make average pressure (p_{avg}) and average velocity (u_{avg}) of a selected sampling region (area for 2D, volume for 3D) satisfy Bernoulli's principle.

$$\boldsymbol{p_{avg} = p_{\infty} + \frac{1}{2\rho}(u_{\infty}^2 - u_{avg}^2)} \qquad \textbf{(6)}$$

5. Select a range of the input data and execute: since 300 images where captured the selected range was 1 to 300 and an increment of 1. Then, started processing which executed Pressure from PIV with the given selected range.

7. RESULTS AND ANALYSIS

Results were calculated for Pressure from PIV with the given Selected range and the images were post processed using DaVis FlowMaster 10.0.4 software. The results were analysed for the five flowrates and eight positions selected for both the input and output test sections and average pressure values computed.

7.1 RESULTS OF VELOCITY FIELDS FOR INLET AND OUTLET TEST SECTIONS

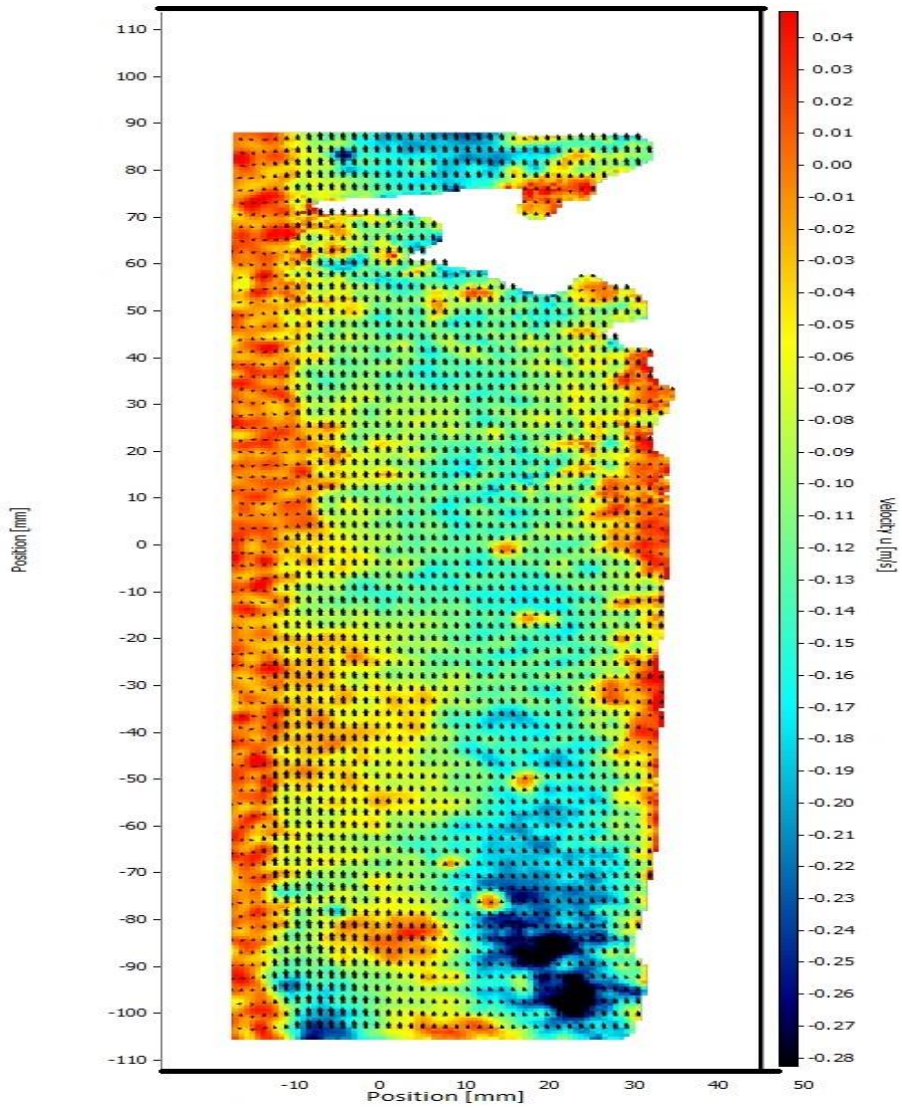

Figure 12: Velocity fields, velocity against position for the inlet test section at 0.019 m^3/s.

The figure above shows the graphical representation of velocity fields for the inlet test section at 0.019 m^3/s. it shows how the velocity is distributed in the test channel and has can been seen the highest velocity in the flow channel is 0.04 m/s and lowest is – 0.28 m/s. The negative velocity is caused by errors due to particles which are not tracked or lost and create what is termed as ghost particles. The maximum velocity is much on the lining of the channel and the minimum spread evenly mostly on the middle of the channel. The velocity vectors clearly show that the flow in the test section is from bottom to top.

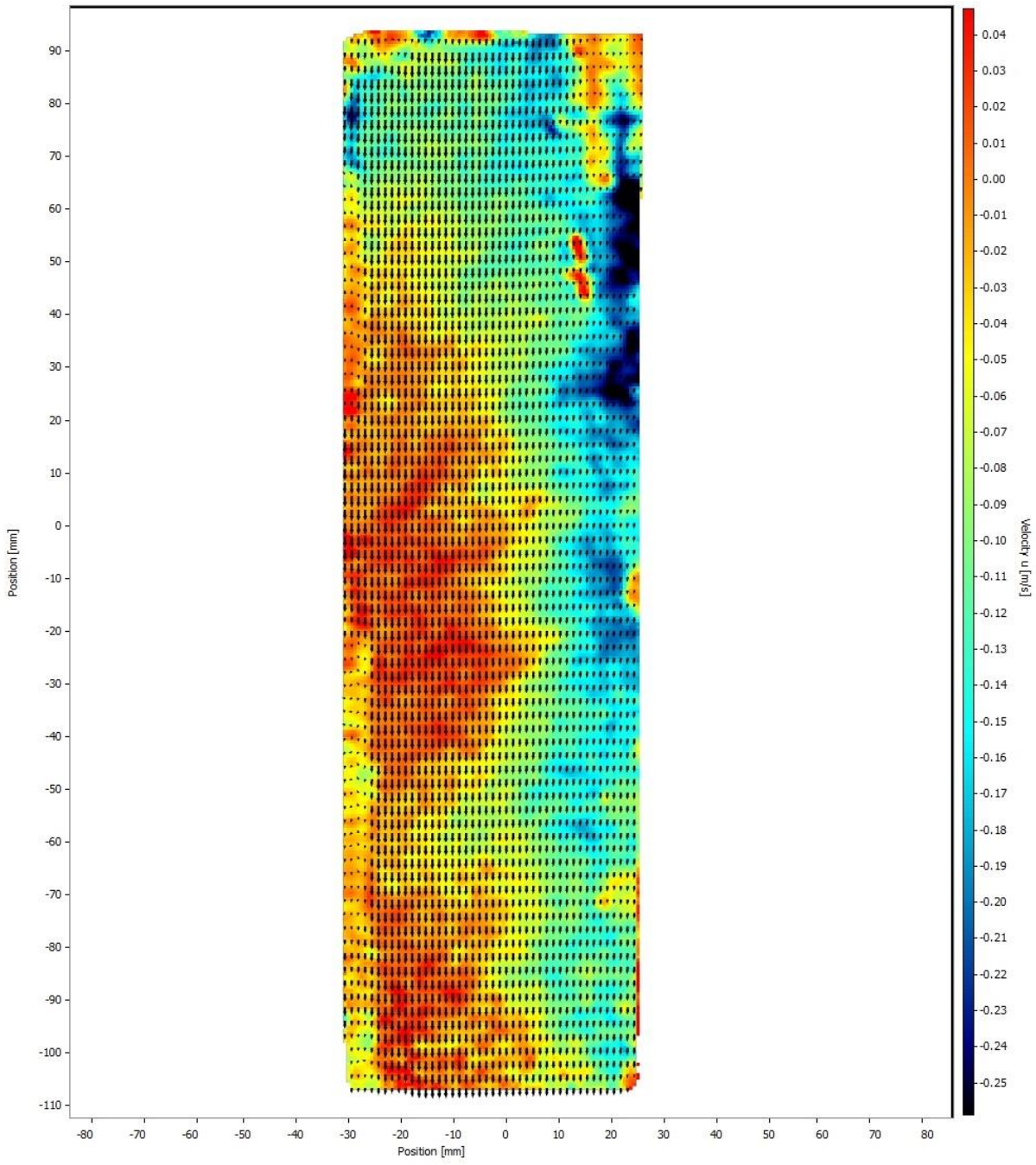

Figure 13: Velocity fields, velocity against position for outlet test section at 0.019 m^3/s.

The figure above shows the graphical representation of velocity fields, for the outlet test section at 0.019 m^3/s, has you can notice the highest velocity in the flow channel is 0.04 m/s and lowest is – 0.25 m/s. As the gas particle move and collide with another and against the elbow the velocity vectors clearly shows that the flow in the test section is from top to bottom, thereby agreeing with the basic laws of flow since the diameter of the two cross section testing section are the same. (Continuity) conservation of mass.

7.2 PRESSURE FIELDS FROM VELOCITY FIELDS.

As earlier mentioned, Pressure from PIV reconstructs pressure fields from velocity fields. Below are the two pressure fields for the inlet and outlet test section for the highest flow rate;

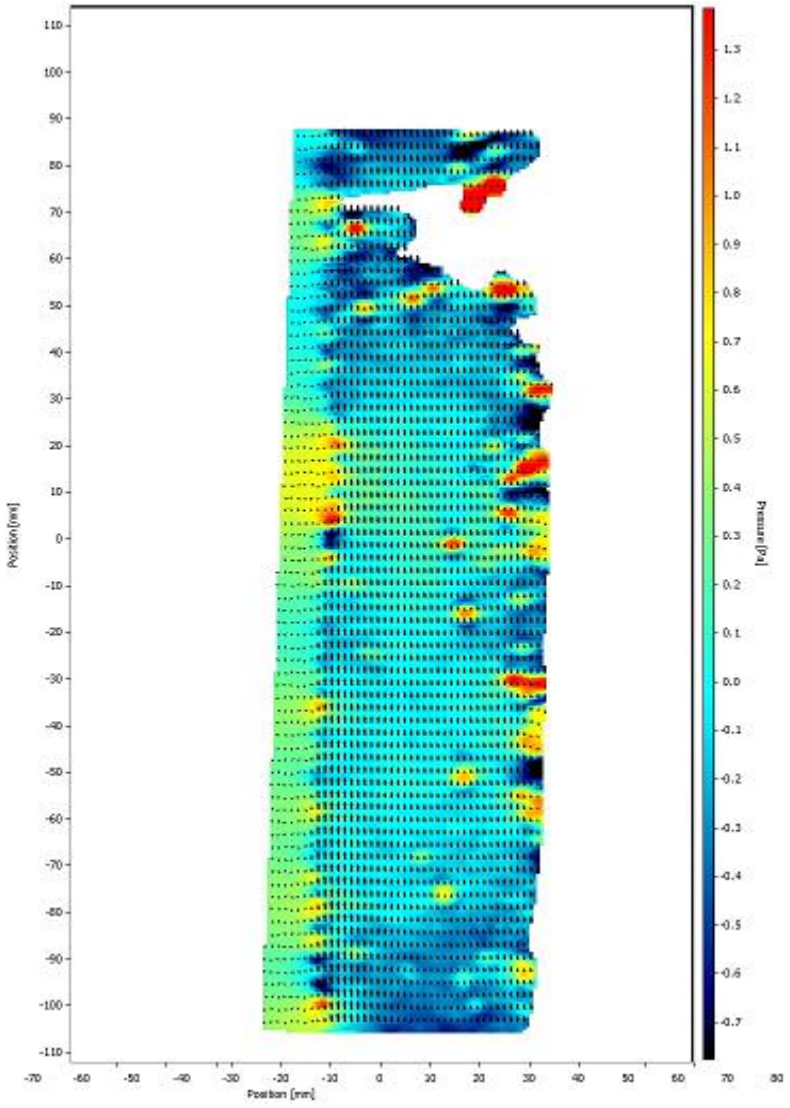

Figure 14: Pressure fields for the inlet test section, pressure against position.

The figure above shows the pressure fields for the highest flowrate of 0.019 m^3/s reconstructed from the velocity field of ***Figure 12***. The pressure fields are evaluated from the velocity fields using the

pressure-based PIV – Bernoulli's equation with the high pressure of 1.3 Pa and lowest of -0.7 Pa. A fluid always flows from a higher total energy zone to a lower total energy zone.

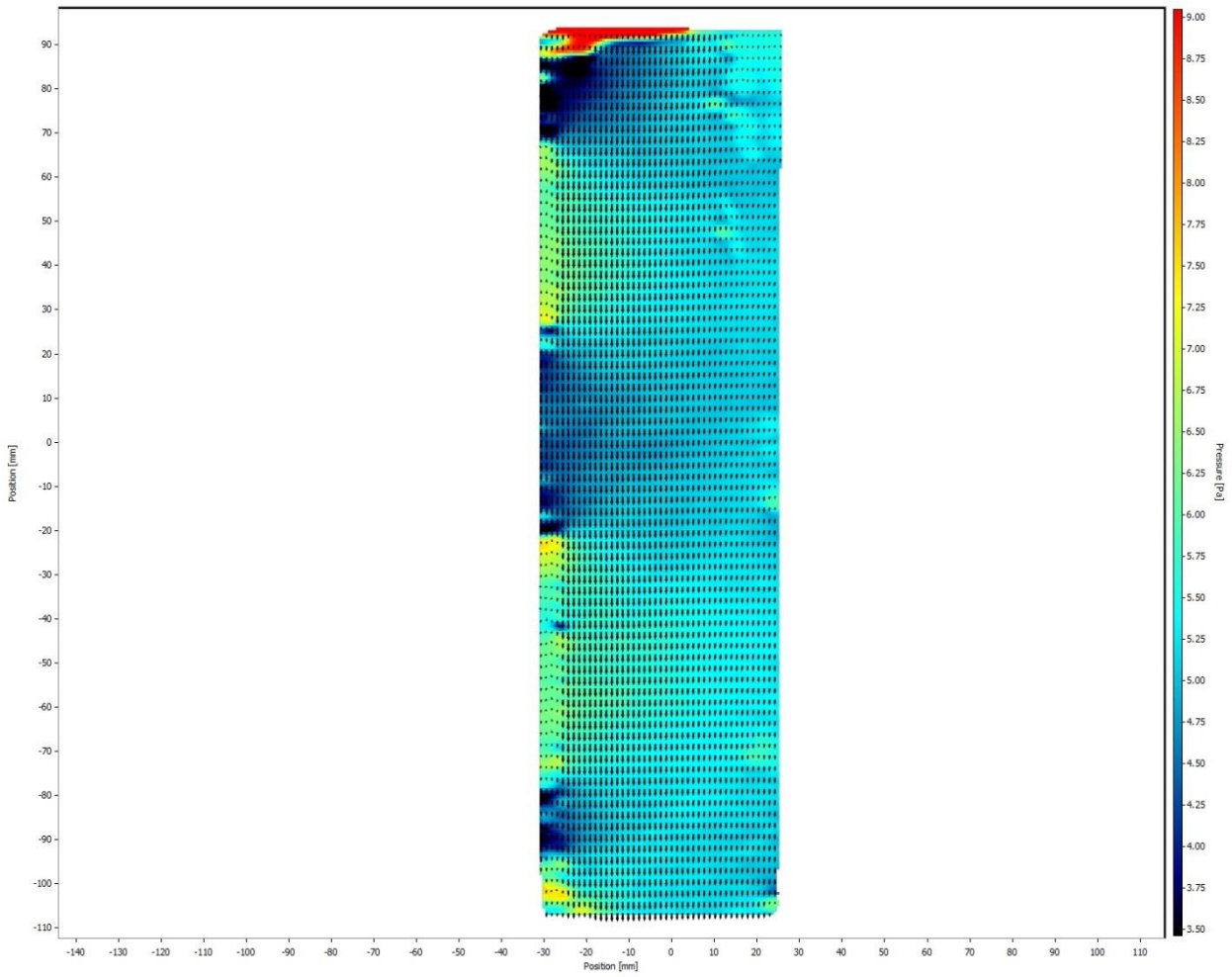

Figure 15: Pressure fields for the outlet test section, pressure against

As can be seen the highest pressure (9 Pa) is just near the top entry for the outlet test section, this could be because as the fluid moves some change in momentum is observed as the gas particles hits into the elbow and also due to change in direction. When the gas moves as a whole, the measured pressure changes in the direction of the movement. The gas's ordered motion provides an ordered component of momentum in the motion's direction. This fluid momentum is associated with an additional pressure component known as dynamic pressure. The total pressure is equal to the sum of the static and dynamic pressures, as stated by Bernoulli's equation, and is measured in the direction of motion

During my evaluation I took the average pressure values greater than zero because the zero values were not important for the purpose of this thesis.

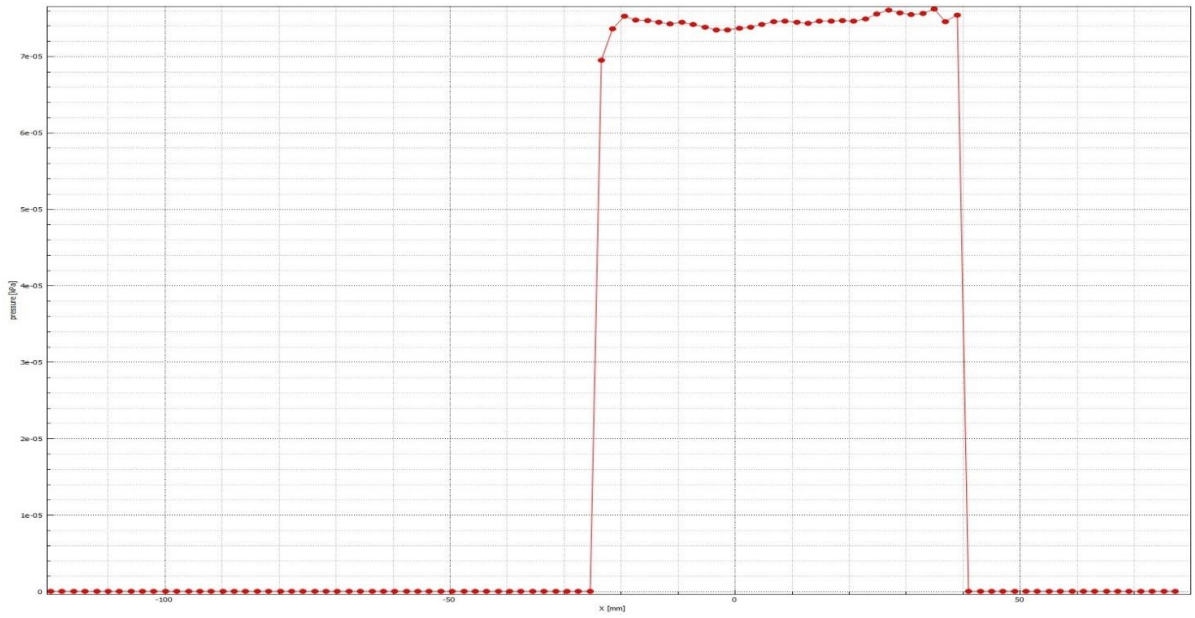

Figure 16: Pressure values at point 1 showing the reason of leaving out zero values and averaging values above zero to get the pressure at point 1.

After evaluation of the average pressure values for eight selected points from both the inlet and outlet test section for the all the five measured flowrates, the relation of pressure against position was plotted and the figure below shows the pressure decreasing as we move from bottom to top from the inlet side and top to bottom from outlet side. The positive value of change in pressure (dp) indicates that the inlet pressure is greater than the outlet pressure, so pressure will decrease by 0.09 Pa from position 1 to 2, drops by 0.2 Pa from position 2 to 3 solely due to the change in elevation of the fluid as it flows uphill as can be seen in the graph and table below;

Table 2: Pressure at different positions for different variants

POSITION	V01 (Pa)	V02 (Pa)	V03 (Pa)	V04 (Pa)	V05 (Pa)
1	7.310846	1.830066	1.08680875	8.45E-02	2.43E-02
2	7.222817	1.793173	1.053584938	8.03E-02	2.39E-02
3	7.005699	1.740317	1.050269719	8.16E-02	2.30E-02
4	6.8764	1.696275	1.050202813	7.90E-02	2.24E-02
5	5.558177	1.347416	0.936937375	7.45E-02	2.10E-02
6	4.957529	1.227426	0.731005398	6.81E-02	2.00E-02
7	5.452666	1.211101	0.646977	6.73E-02	1.99E-02
8	5.243176	1.190235	0.605248795	6.57E-02	1.96E-02

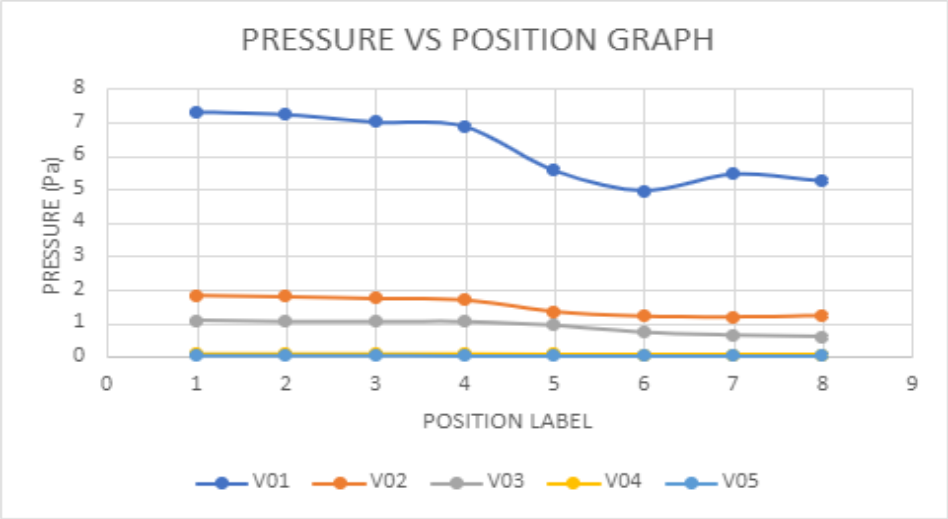

Figure 17: Pressure against position

The **figure 20** below shows points 1-4 for the inlet test section, from the first elbow. Points 5-8 are for the outlet test section, same distances. The data was then sorted in the flow direction. The dimensionless pressure was calculated, which is the pressure value divided by the maximum for each flow rate (inlet velocity). Below shows the relationship

Table 3: Dimensionless pressure for different variants

POSITION	V01	V02	V03	V04	V05
1	1	1	1	1.00E+00	1.00E+00
2	0.987959123	0.979840618	0.969429936	9.50E-01	9.84E-01
3	0.958261055	0.950958599	0.966379521	9.66E-01	9.47E-01
4	0.94057514	0.926892801	0.966317958	9.35E-01	9.22E-01
5	0.760264544	0.736266342	0.862099587	8.81E-01	8.62E-01
6	0.678106063	0.670700401	0.672616408	8.06E-01	8.21E-01
7	0.745832425	0.661779958	0.595299771	7.96E-01	8.18E-01
8	0.717177738	0.650378183	0.556904603	7.77E-01	8.04E-01

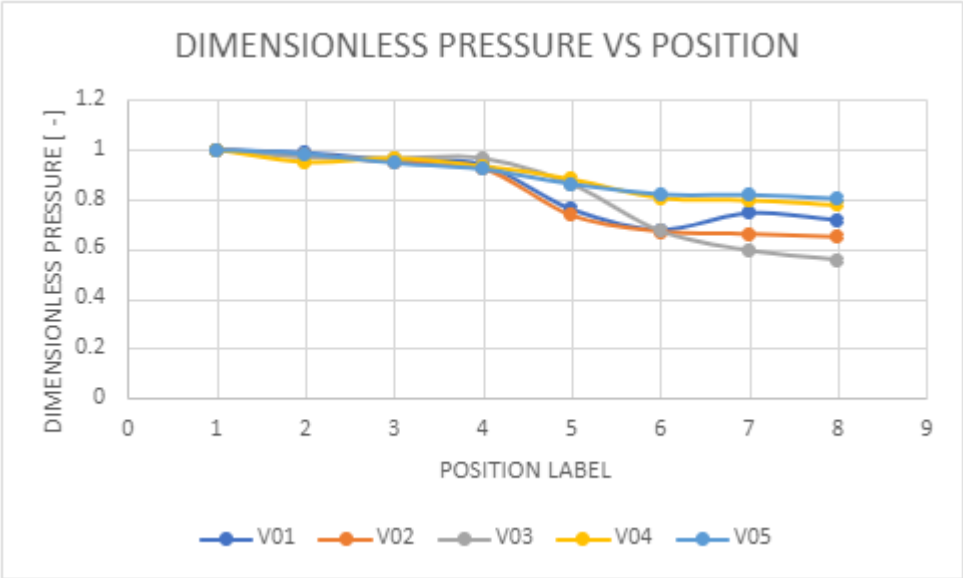

Figure 18: Dimensionless Pressure against position

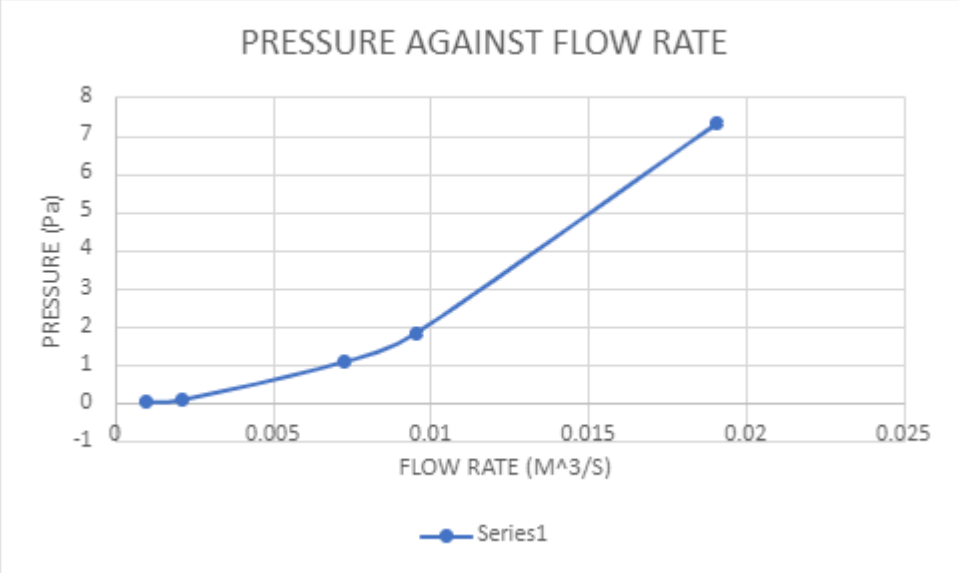

Figure 19: Pressure against flow rate

The graph above shows the resulting pressure drop for the gas at 26 degrees Celsius over a range of flow rates for the 80 mm diameter cylindrical pipe test section.

8. CONCLUSION

From the presented results the highest measured pressure is about 9 Pascals which is close to pressure characteristics of the elbow used (i.e.., 10 Pa - 12 Pa for the velocity of 3.8 m/s). we can also conclude that, a fluid always flows from a higher total energy zone to a lower total energy zone. When the gas moves as a whole, the measured pressure changes in the direction of the movement. The gas's ordered motion provides an ordered component of momentum in the motion's direction. This fluid momentum is associated with an additional pressure component known as dynamic pressure. The total pressure is equal to the sum of the static and dynamic pressures, as stated by Bernoulli's equation, and is measured in the direction of motion. It's worth noting that a fluid's pressure drop is proportional to both the velocity value and the gradient of the velocity. The form of the dynamic pressure in Bernoulli's Equation is determined by solving the momentum equation. A drop in pressure can be caused by a change in elevation; an increase in velocity can be caused by a change in velocity. The overall effect will be determined by the magnitudes of each alteration. If the change in elevation or velocity results in a pressure increase larger than the static pressure of the fluid, it is possible that the static pressure of the fluid actually increases from input to outlet. Therefore, we can conclude that the pressure-based PIV can be used to evaluate pressure drop in a channel.

8.1. RECOMMENDATIONS

1. When setting boundary condition option for using the Bernoulli's principle, the free-stream velocity and pressure values and a sampling region should be accurately measured and inputted. A selection of the sampling region should be a stable free-stream-like flow. It means that the averaged velocity of the region should not differ by more or less than 15% of free-stream velocity.

2. Stereoscopic PIV should be employed because Planar PIV has some inherent errors during data capturing due to the perspective transformation, velocity vectors' out of-plane component gets lost, while an unrecoverable error impacts the in-plane components.

3. Errors caused by reflections should be addressed during data collection; an alternative for internal flows is to construct a model with flat external walls (e.g., a model machined from a rectangular block using acrylic plastic).

4. Measurement should be done with higher flow rates (at least above 0.007 m^3/s) because for lower flow rates it is difficult to clearly see fluid property changes for pressure-based PIV. Basically,

because you have low density in seeding particles (see picture for velocity and pressure fields for the lowest flowrate at the appendix)

REFERENCE

[1] FRENZEL, F, H GROTHEY, C HABERSETZER, M HIATT, W HOGREFE, M KIRCHNER, G LÜTKEPOHL, W MARCHEWKA, U MECKE a M OHM. Industrial flow measurement basics and practice. ABB automation products Gmbh. 2011, 290.

[2] EDITION, Fourth. of Fluid Mechanics. nedatováno. ISBN 047144250X.

[3] ERIC - EJ935038 - Gas Pressure-Drop Experiment, Chemical Engineering Education, 2010 [online]. [vid. 2021-06-01]. Dostupné z: https://eric.ed.gov/?id=EJ935038

[4] VAN OUDHEUSDEN, B. W. PIV-based pressure measurement. Measurement Science and Technology [online]. 2013, **24**(3). ISSN 13616501. Dostupné z: doi:10.1088/0957-0233/24/3/032001

[5] WIENEKE, Bernhard. PIV uncertainty quantification from correlation statistics. Measurement Science and Technology [online]. 2015, **26**(7), 074002. ISSN 13616501. Dostupné z: doi:10.1088/0957-0233/26/7/074002

[6] C Greated, J Cosgrove, JM Buick. Optical Methods for Data Processing in Heat & Fluid flow. 2002, **53**(9), 1689–1699. ISSN 1098-6596.

[7] SHEN, Weijun, Fuquan SONG, Xiao HU, Genmin ZHU a Weiyao ZHU. Experimental study on flow characteristics of gas transport in micro- and nanoscale pores. Scientific Reports [online]. 2019, **9**(1), 1–10. ISSN 20452322. Dostupné z: doi:10.1038/s41598-019-46430-2

[8] TANG, G. H. a Y. L. HE. An experimental investigation of gaseous flow characteristics in microchannels. Proceedings of the Second International Conference on Microchannels and Minichannels (ICMM2004) [online]. 2004, **3954**, 359–366. Dostupné z: doi:10.1115/icmm2004-2356

[9] FUJISAWA, N, S LIU a T YAMAGATA. Numerical study on ignition and failure mechanisms of hydrogen explosion accident in Fukushima Daiichi Unit 1. Engineering Failure Analysis [online]. 2021, **124**, 105388. Dostupné z: doi:10.1016/j.engfailanal.2021.105388

[10] KEANE, R. D. a R. J. ADRIAN. Optimization of particle image velocimeters. I. Double

pulsed systems. Measurement Science and Technology [online]. 1990, **1**(11), 1202–1215. ISSN 09570233. Dostupné z: doi:10.1088/0957-0233/1/11/013

[11] ELSINGA, G. E., F. SCARANO, B. WIENEKE a B. W. VAN OUDHEUSDEN. Tomographic particle image velocimetry. Experiments in Fluids [online]. 2006, **41**(6), 933–947. ISSN 07234864. Dostupné z: doi:10.1007/s00348-006-0212-z

[12] Newtonian and Non-Newtonian Fluids - Engineered Software Knowledge Base [online]. [vid. 2021-05-31]. Dostupné z: http://kb.eng-software.com/eskb/ask-an-engineer/fluid-property-questions/newtonian-and-non-newtonian-fluids

[13] FLOW IN PIPES. nedatováno.

[14] WALEED ABED, Assist M. Fluid Mechanics Course Tutor Handout Lectures for Year Two Chapter Five/ Flow i n pipes. nedatováno.

[15] What is Bernoulli's equation? (article) | Khan Academy [online]. [vid. 2021-06-02]. Dostupné z: https://www.khanacademy.org/science/physics/fluids/fluid-dynamics/a/what-is-bernoullis-equation

[16] Law of Hagen-Poiseuille — CARPentry documentation [online]. [vid. 2021-06-06]. Dostupné z: https://carpentry.medunigraz.at/examples/tutorials/tutorials.06_fluid.01_HagenPouseille_Stationary.run.html

[17] FlowMaster Pressure from PIV [online]. [vid. 2021-06-02]. Dostupné z: https://www.smart-piv.com/en/applications/fluid-mechanics/pressure_from_piv/index.php

[18] ITTC-Recommended Procedures and Guidelines Guideline on Best Practices for the Applications of PIV/SPIV in Towing Tanks and Cavitation Tunnels ITTC Quality System Manual Recommended Procedures and Guidelines Guideline Guideline on Best Practices for the Applications of PIV/SPIV in Towing Tanks and Cavitation Tunnels. 2017.

[19] MCLACHLAN, B. G., J. L. KAVANDI, J. B. CALLIS, M. GOUTERMAN, E. GREEN, G. KHALIL a D. BURNS. Surface pressure field mapping using luminescent coatings. Experiments in Fluids: Experimental Methods and their Applications to Fluid Flow [online]. 1993, **14**(1), 33–41. ISSN 14321114. Dostupné z: doi:10.1007/BF00196985

[20] KLEIN, Christian, Rolf H. ENGLER, Ulrich HENNE a Werner E. SACHS. Application of pressure-sensitive paint for determination of the pressure field and calculation of the forces and moments of models in a wind tunnel. Experiments in Fluids [online]. 2005, **39**(2), 475–

483. ISSN 07234864. Dostupné z: doi:10.1007/s00348-005-1010-8

[21] AOE 3054 Experiment #4 Particle Image Velocimetry [online]. [vid. 2021-06-02]. Dostupné z: http://www.dept.aoe.vt.edu/~aborgolt/aoe3054/manual/expt4/text.html

[22] LaVision [online]. [vid. 2021-06-01]. Dostupné z: https://www.lavision.de/en/

[23] (PDF) A Review in Particle Image Velocimetry Techniques (Developments and Applications) [online].[vid. 2021-06-01].Dostupné z: https://www.researchgate.net/publication/339302115_A_Review_in_Particle_Image_Velocimetry_Techniques_Developments_and_Applications

[24] SCARANO, F. Iterative image deformation methods in PIV. Measurement Science and Technology [online]. 2001, **13**(1), R1–R19. ISSN 0957-0233. Dostupné z: doi:10.1088/0957-0233/13/1/201

[25] 1 Imaging Techniques for Flow and Motion Measurement Lecture 5 Lichuan Gui University of Mississippi 2011 Imaging & Recording Techniques. - ppt download [online]. [vid. 2021-06-01]. Dostupné z: https://slideplayer.com/slide/7279067/

[26] ELSINGA, G E, B W VAN OUDHEUSDEN a F SCARANO. Experimental assessment of Tomographic-PIV accuracy. Techniques. 2006, (1993), 26–29.

[27] Flow Induced Vibrations - 1st Edition [online]. [vid. 2021-06-01]. Dostupné z: https://www.elsevier.com/books/flow-induced-vibrations/nakamura/978-0-08-044954-8

[28] DESIGN, Equipment. PIV Investigation of the Bluff Body in Water Diplomová práce PIV Investigation of the Bluff Body in Water Master thesis. 2019.

[29] OL 90° 200 oblouk lisovaný - Ventishop.cz [online]. [vid. 2021-05-30]. Dostupné z: https://www.ventishop.cz/ol-90-200-oblouk-lisovany/?gclid=CjwKCAjw47eFBhA9EiwAy8kzNDFcRQNfCGKEr1K8DRNlyPx4mTN0ePma78MblBscwyC8iFtUgF4XGBoCypQQAvD_BwE

APPENDIX 1

VELOCITY AND PRESSURE FIELDS FOR THE OUTLET TEST SECTION

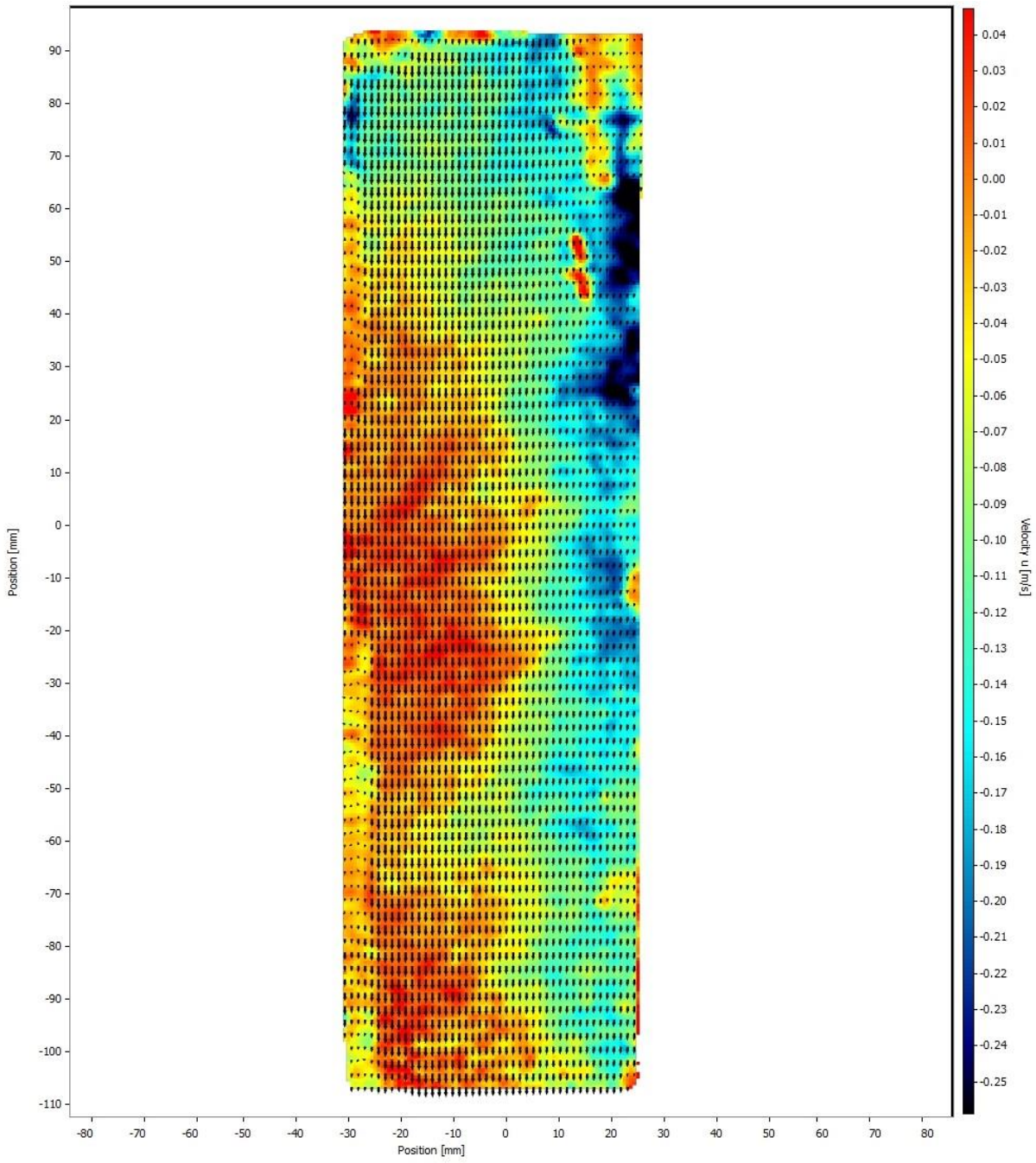

Velocity fields at 0.019 m^3/s

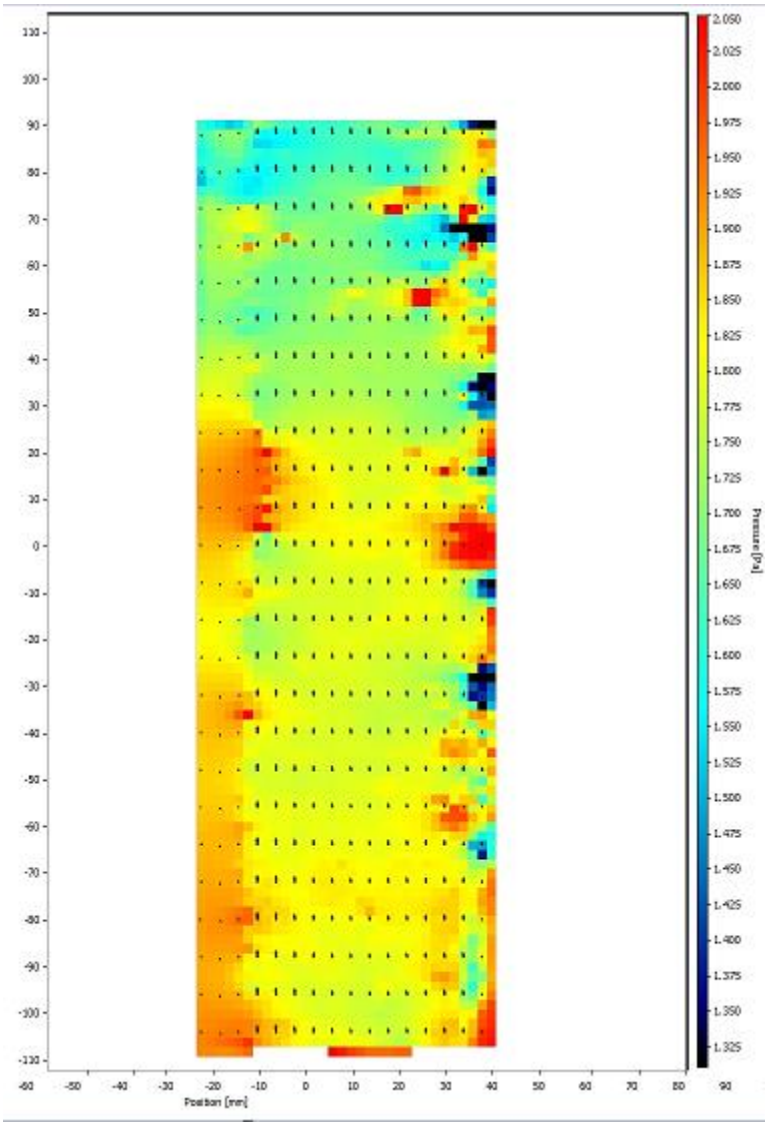

Pressure fields at 3.8 m/s at the outlet test section side

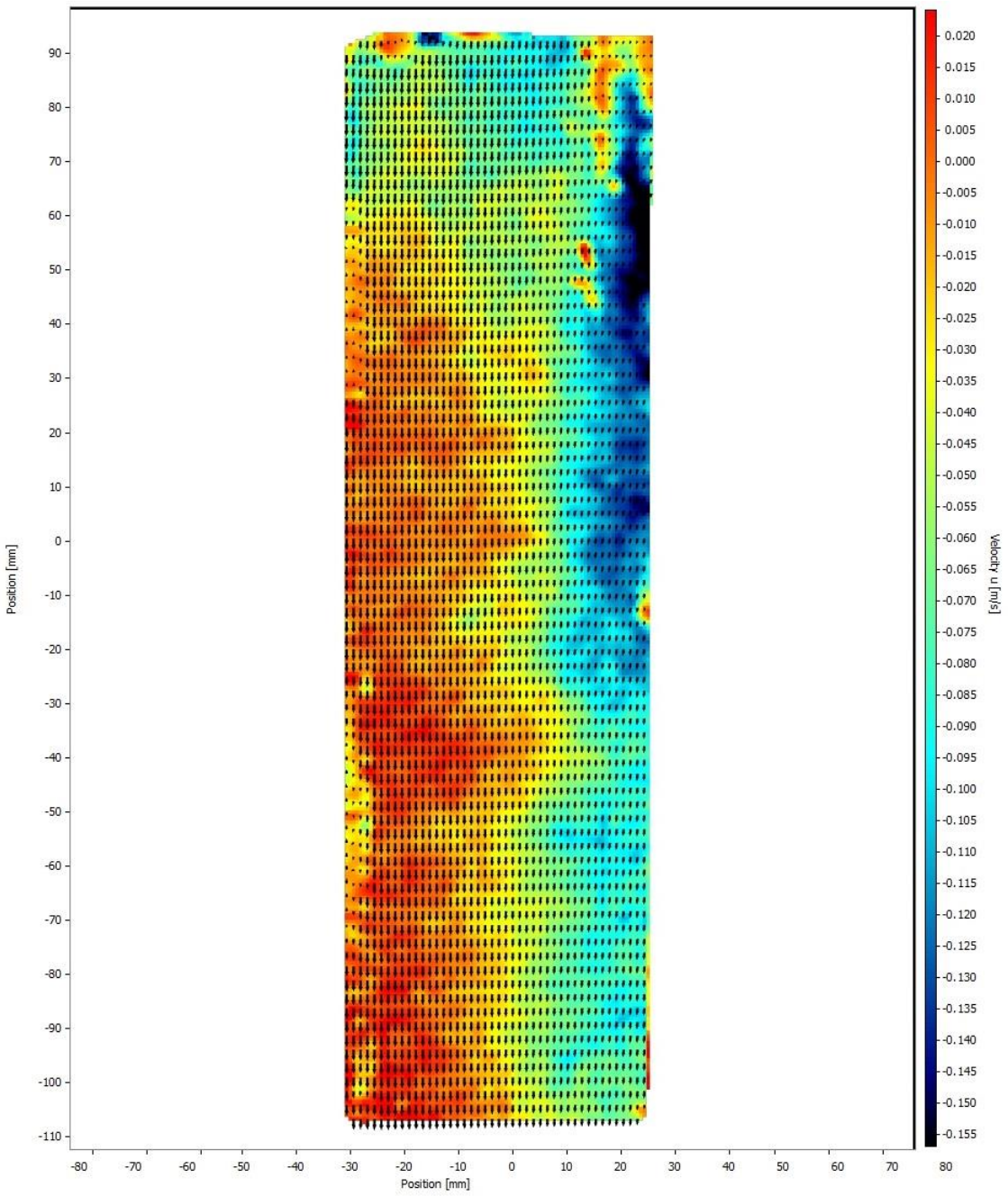

Velocity fields at 0.0086 m^3/s

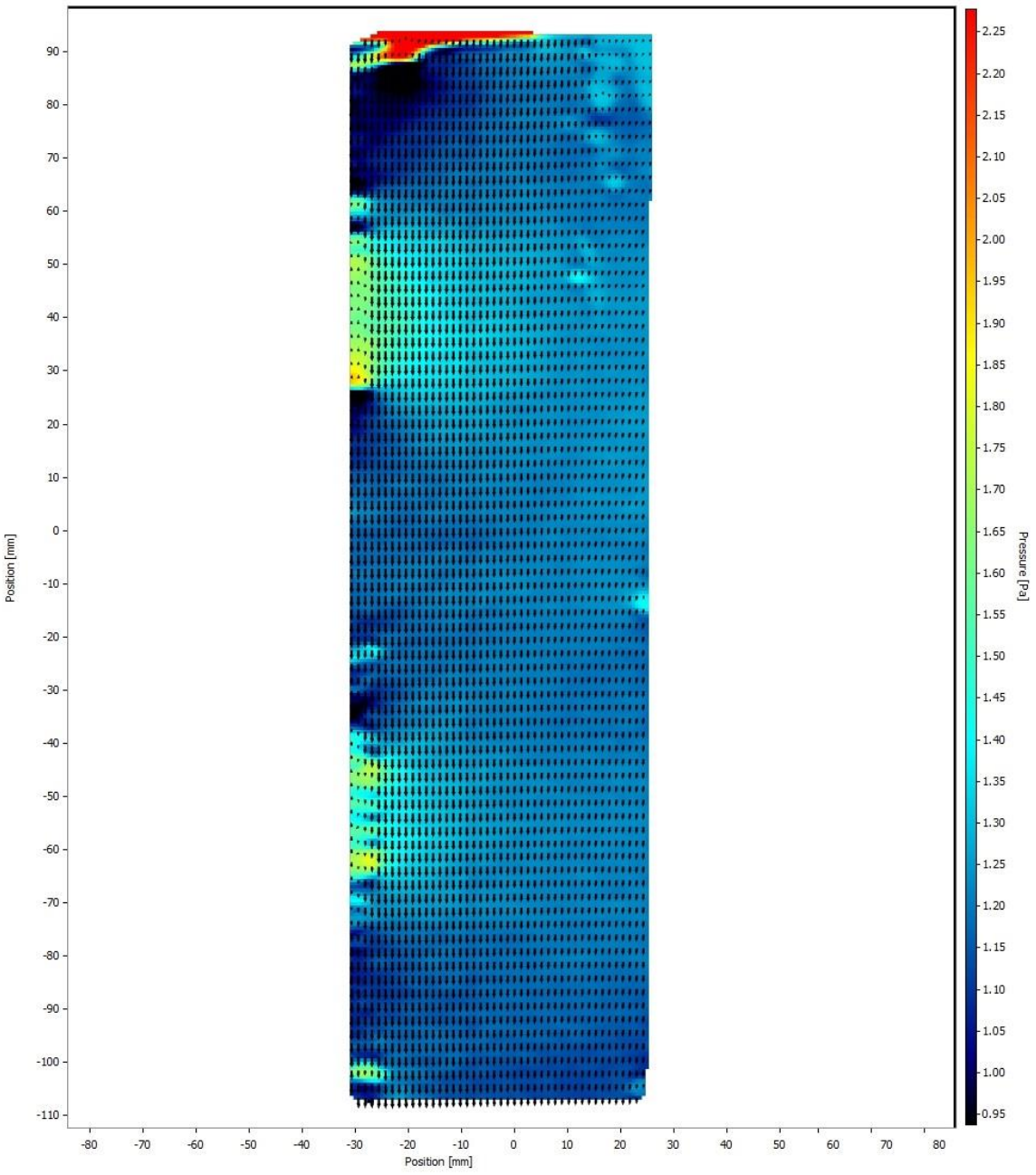

Pressure at 1.9 m/s

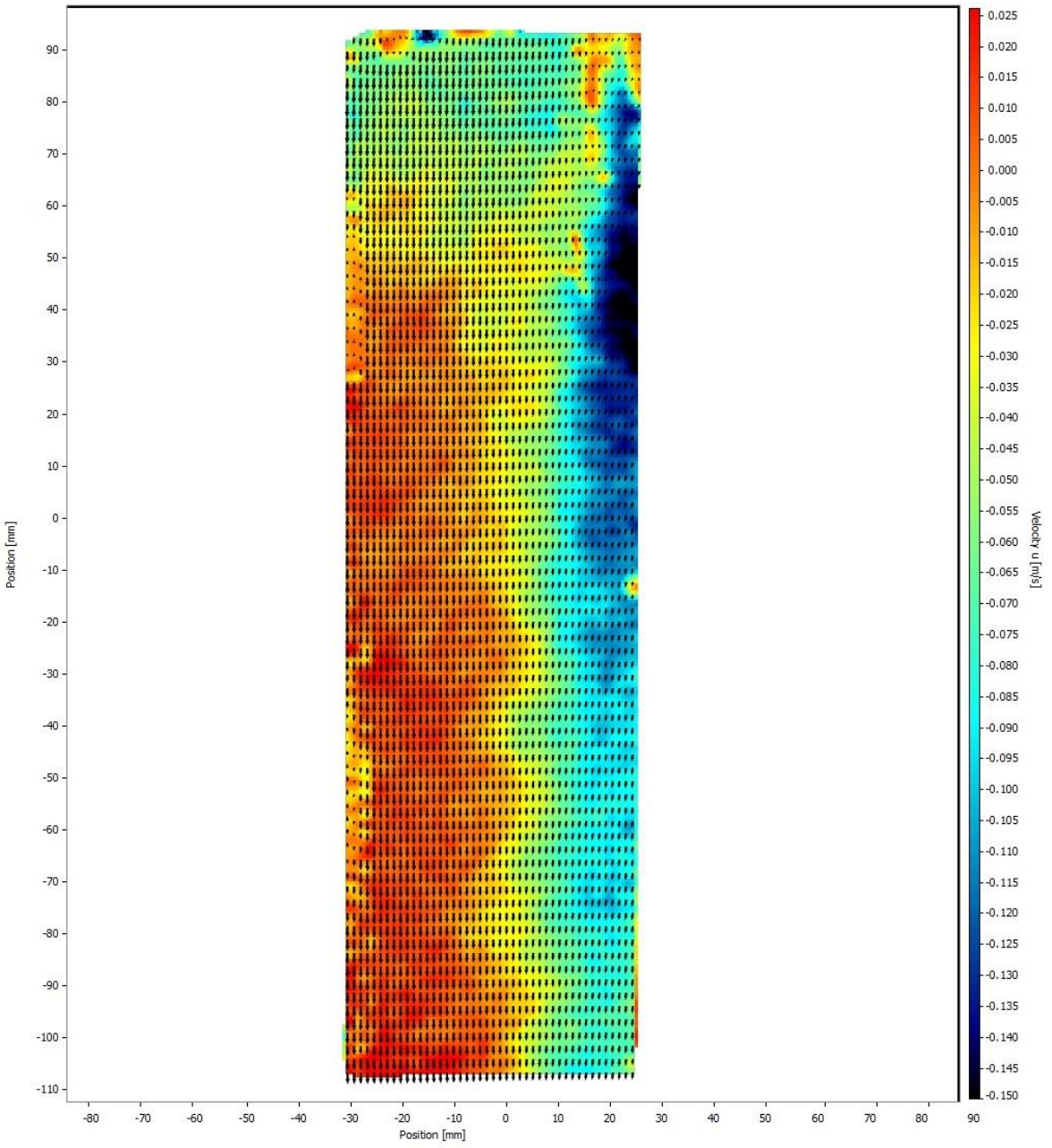

Velocity fields at 0.0073 m^3/s

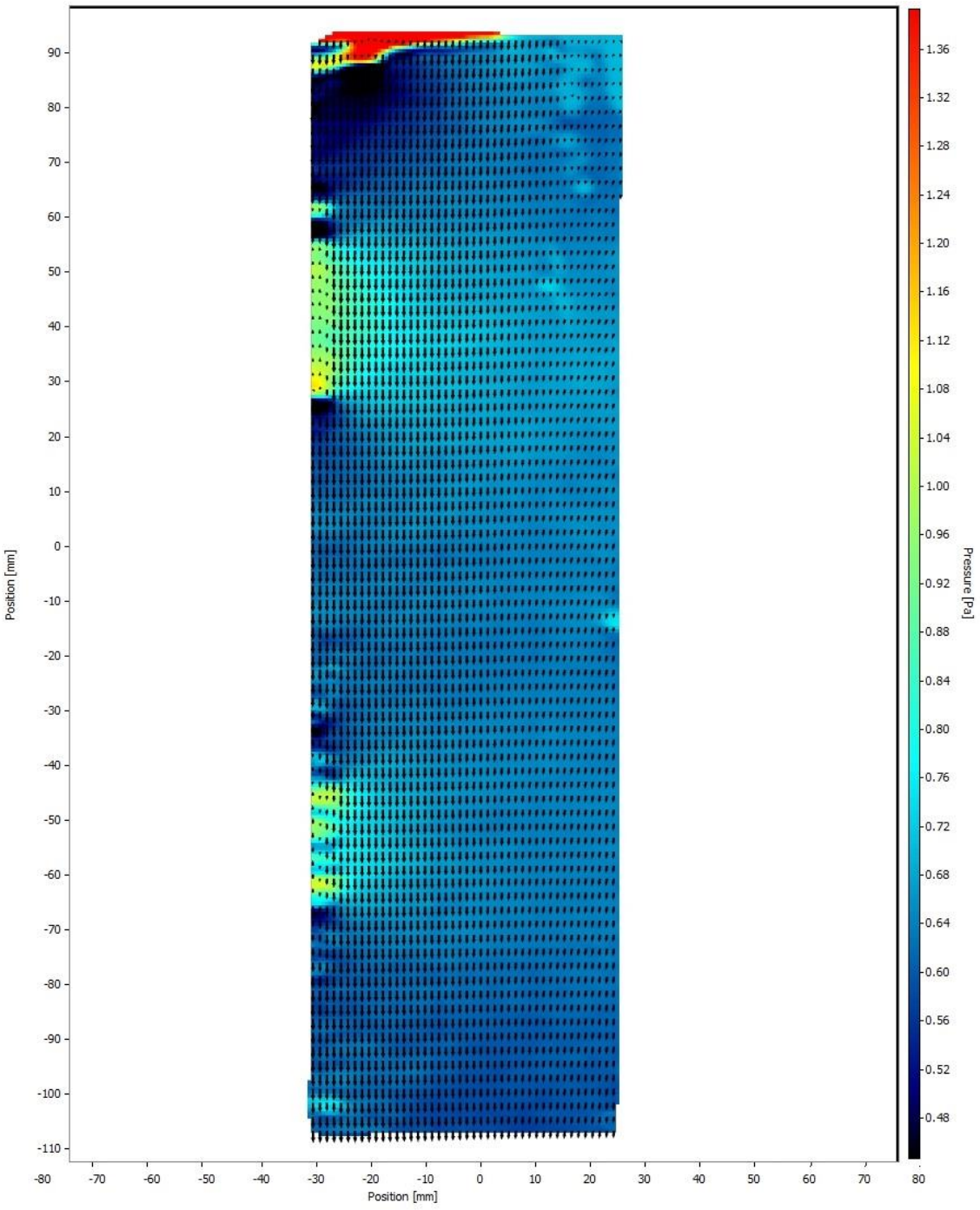

Pressure field at 1.45 m/s

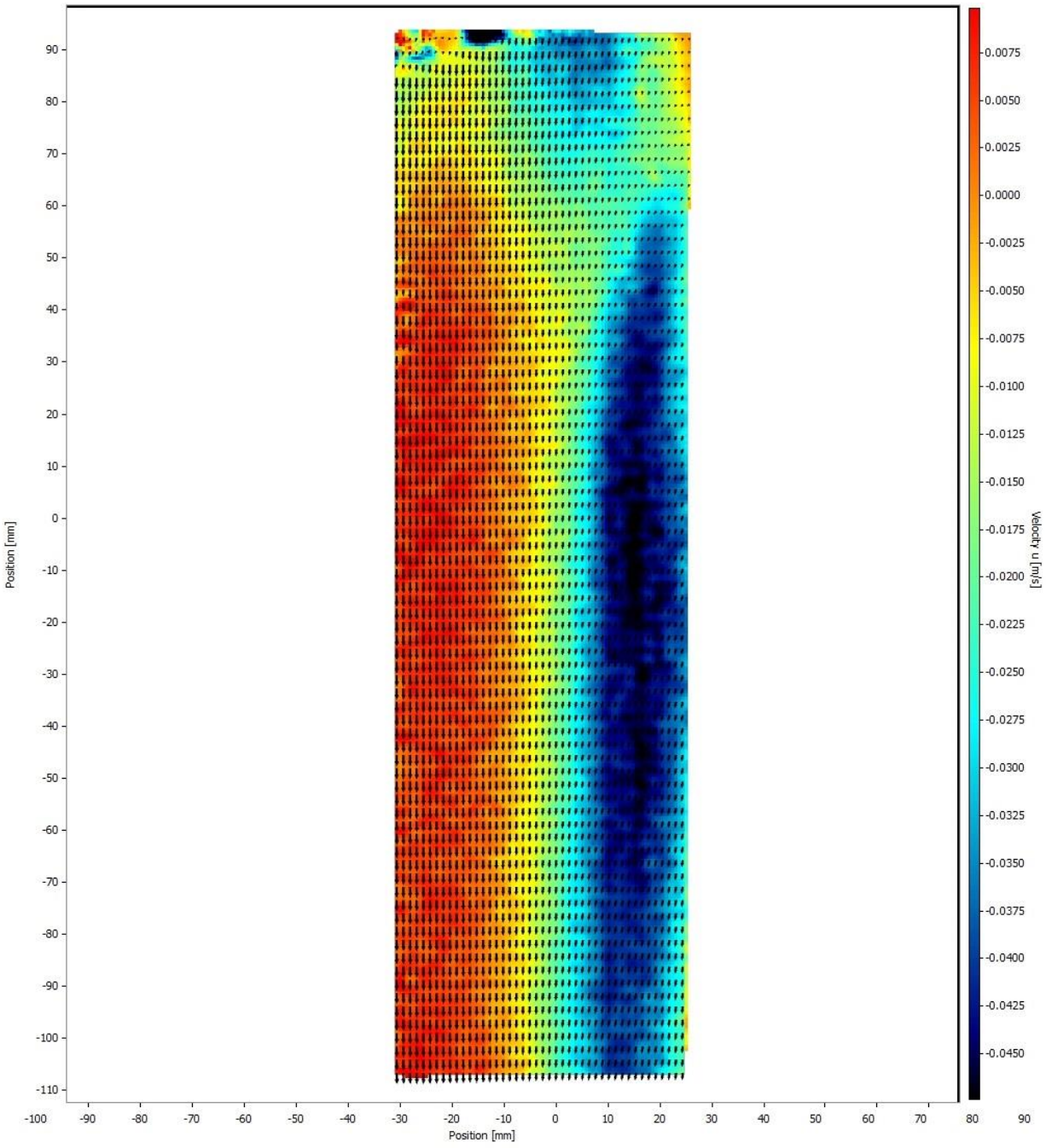

Velocity fields at 0.0021 m^3/s

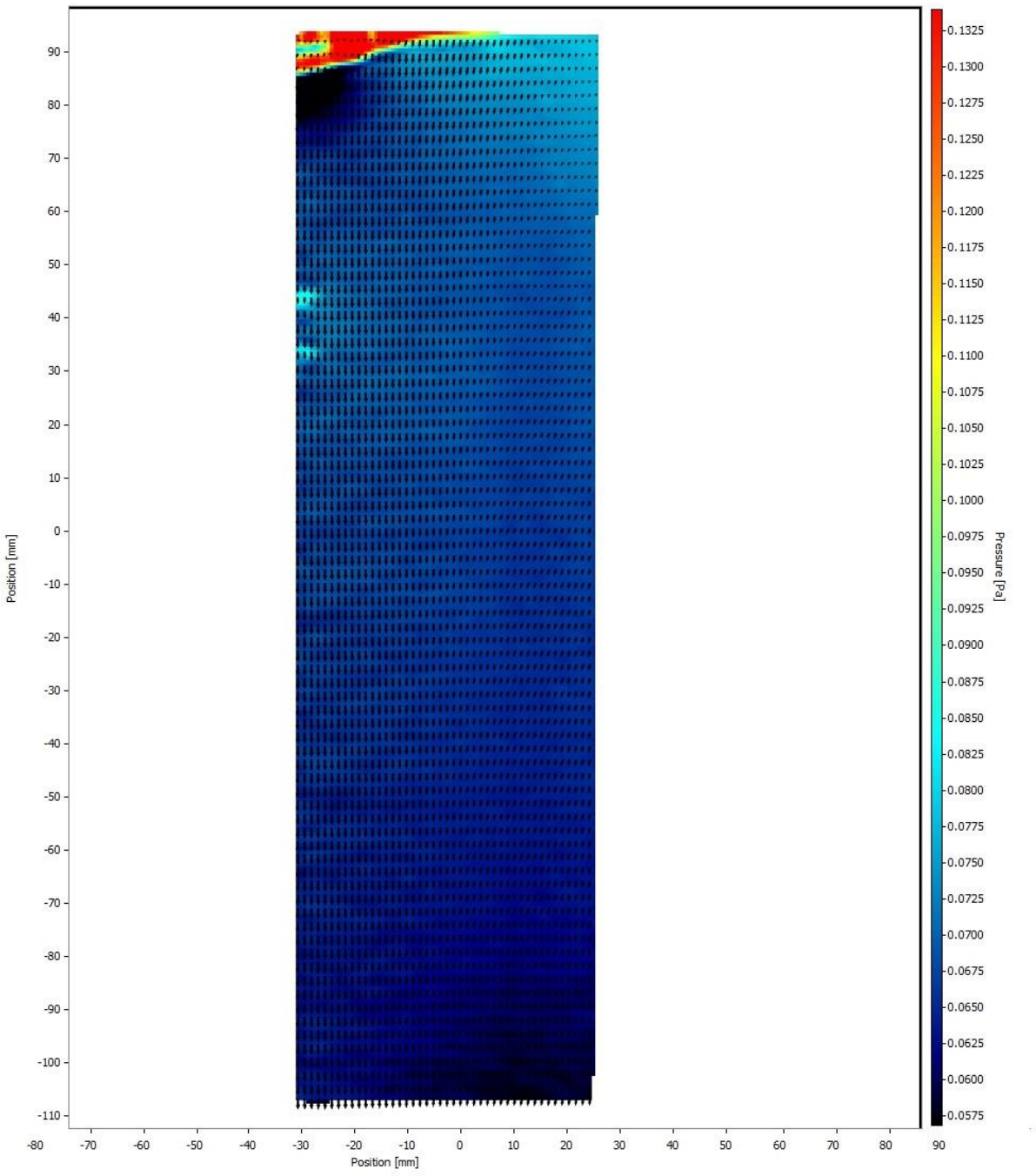

Pressure fields at 0.42 m/s

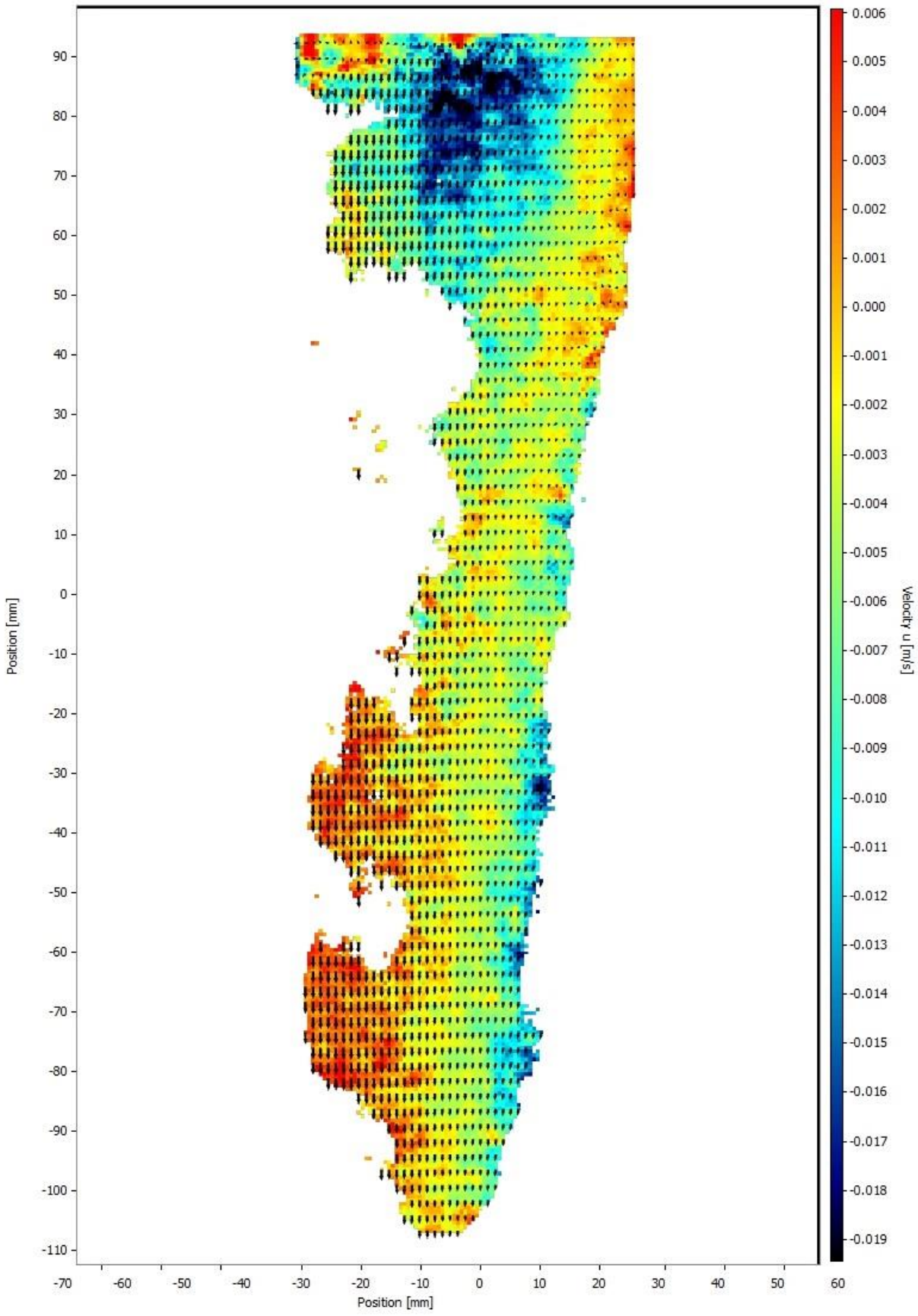

Velocity fields at 0.001 m^3/s

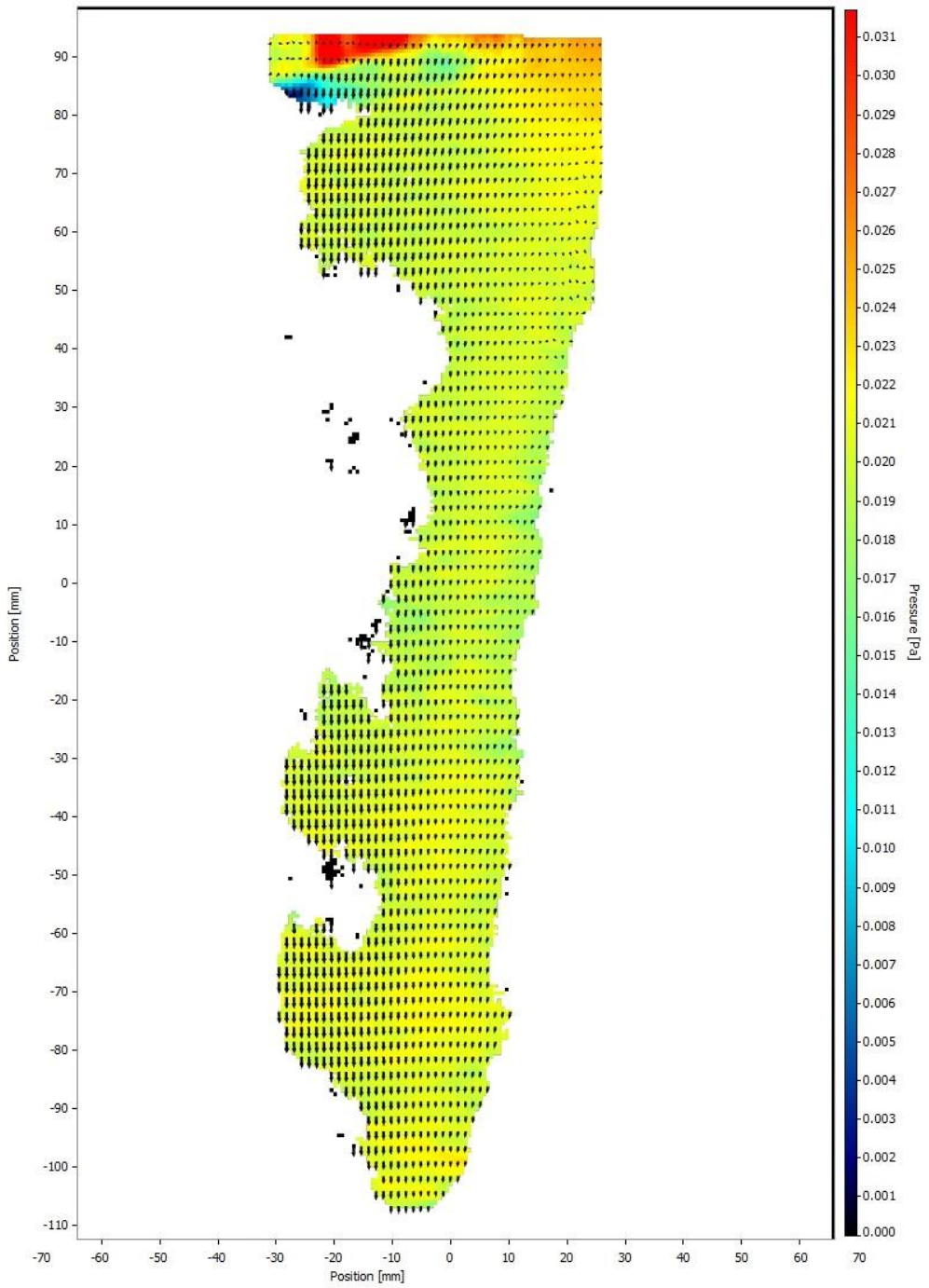

Pressure fields at 0.2 m/s

APPENDIX 2

VELOCITY AND PRESSURE FIELDS FOR THE INLET TEST SECTION

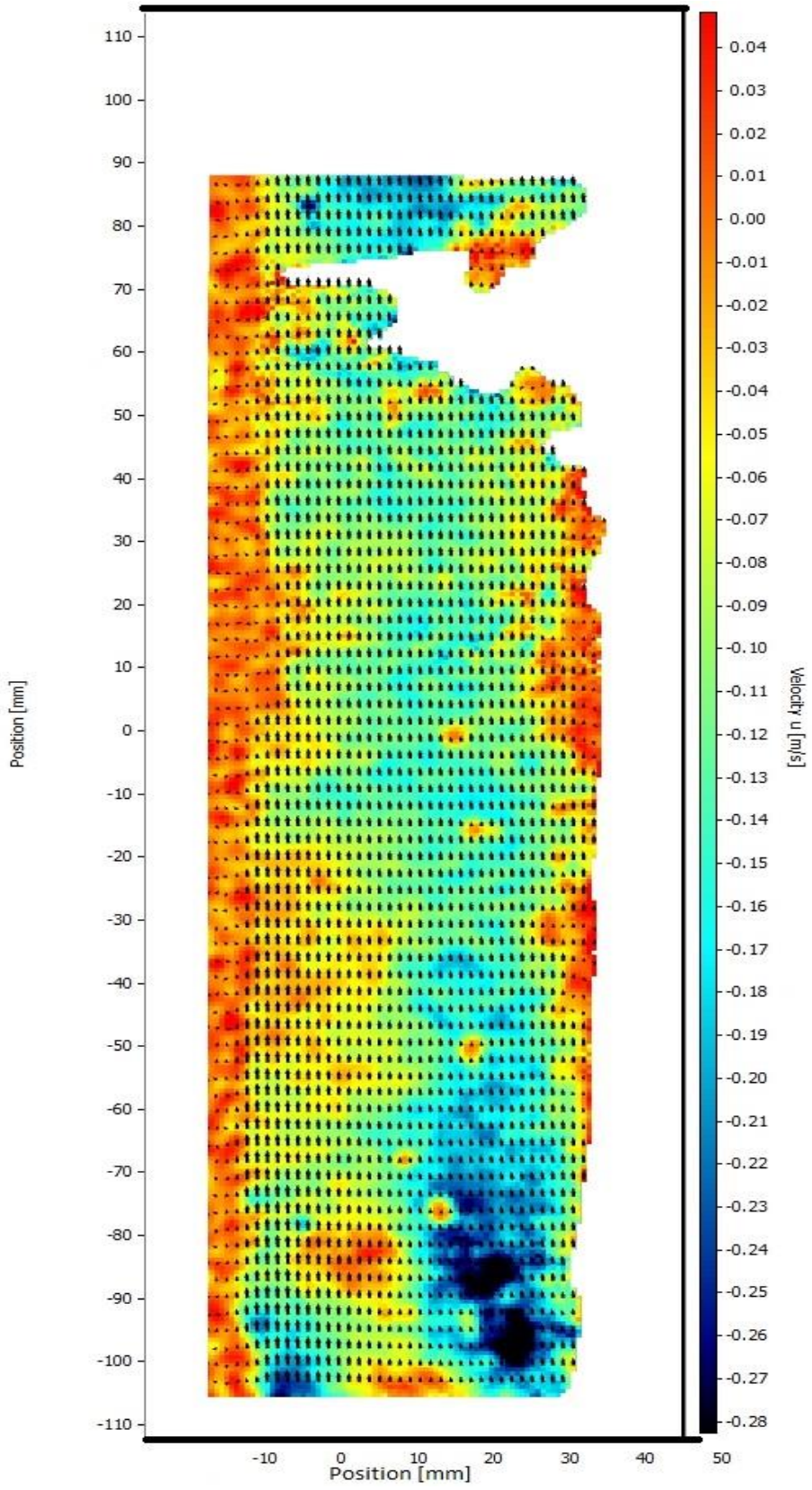

VELOCITY FIELD FOR 0.019 m^3/s

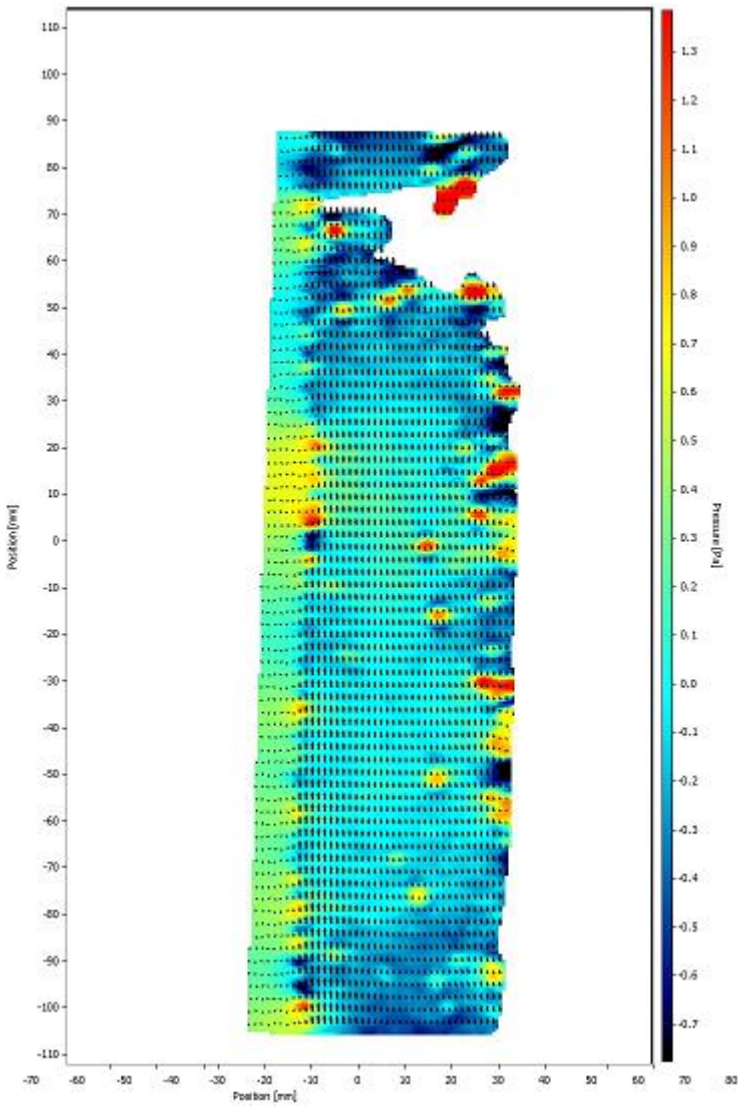

Pressure field for 3.8 m/s

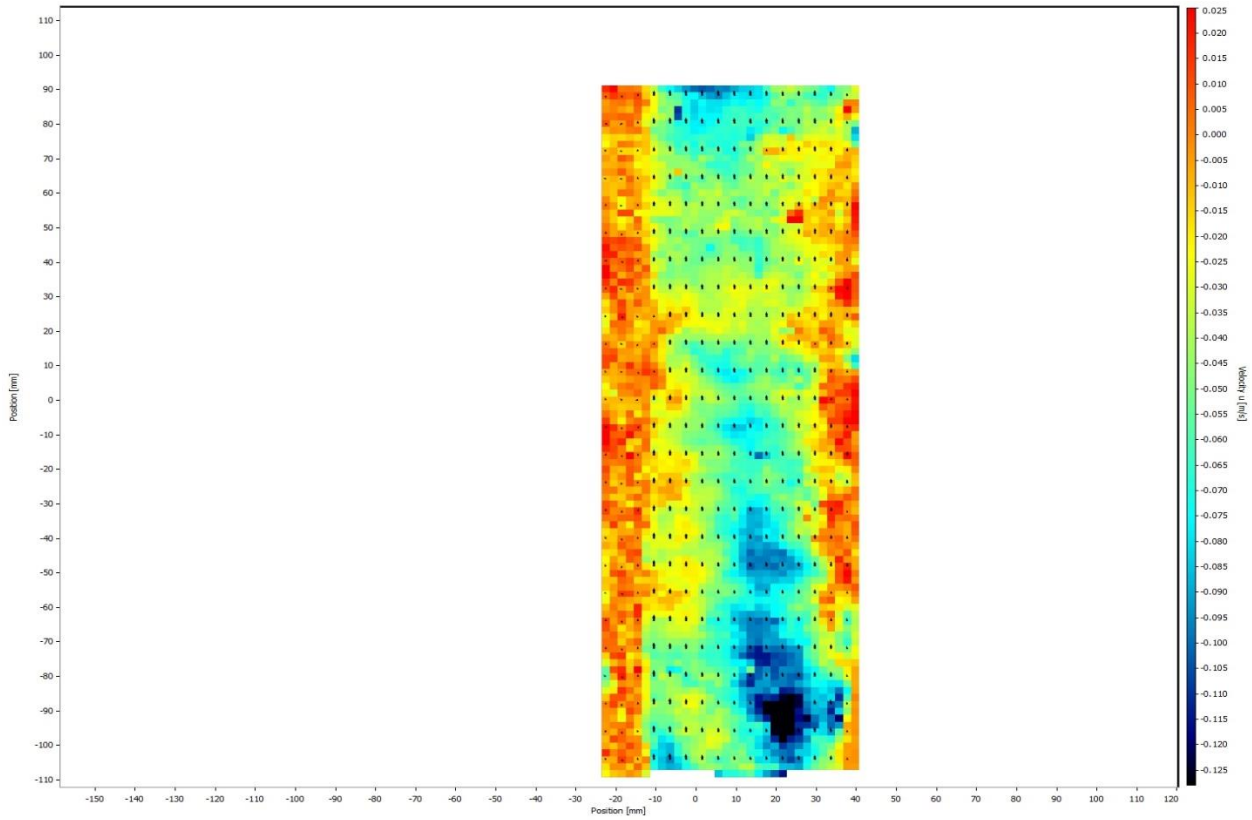

Velocity field at 0.0096 m^3/s

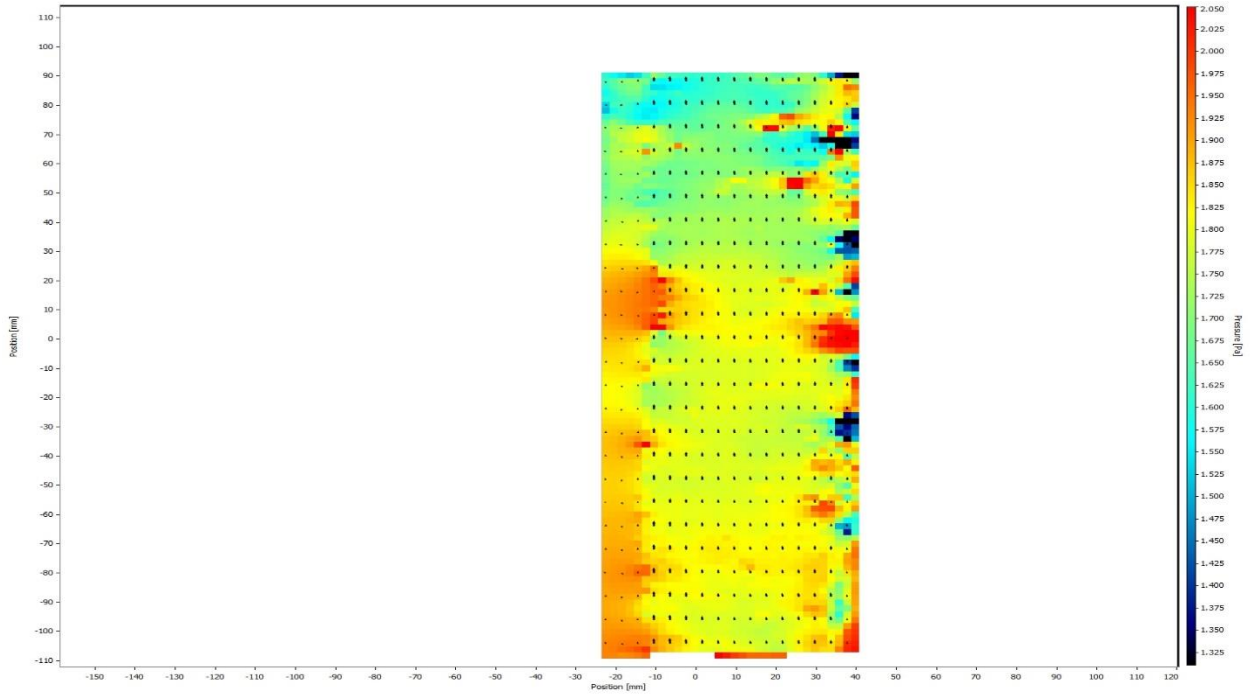

Pressure field for 1.9 m/s

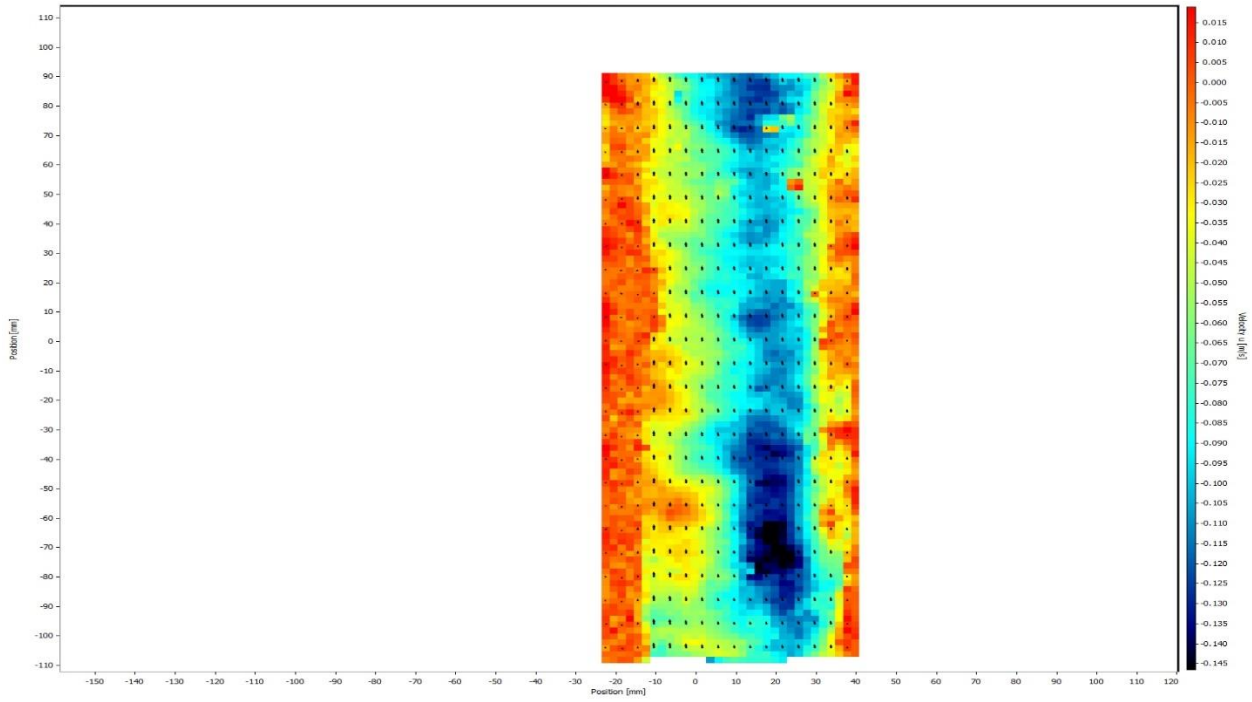

Velocity at 0.073 m^3/s

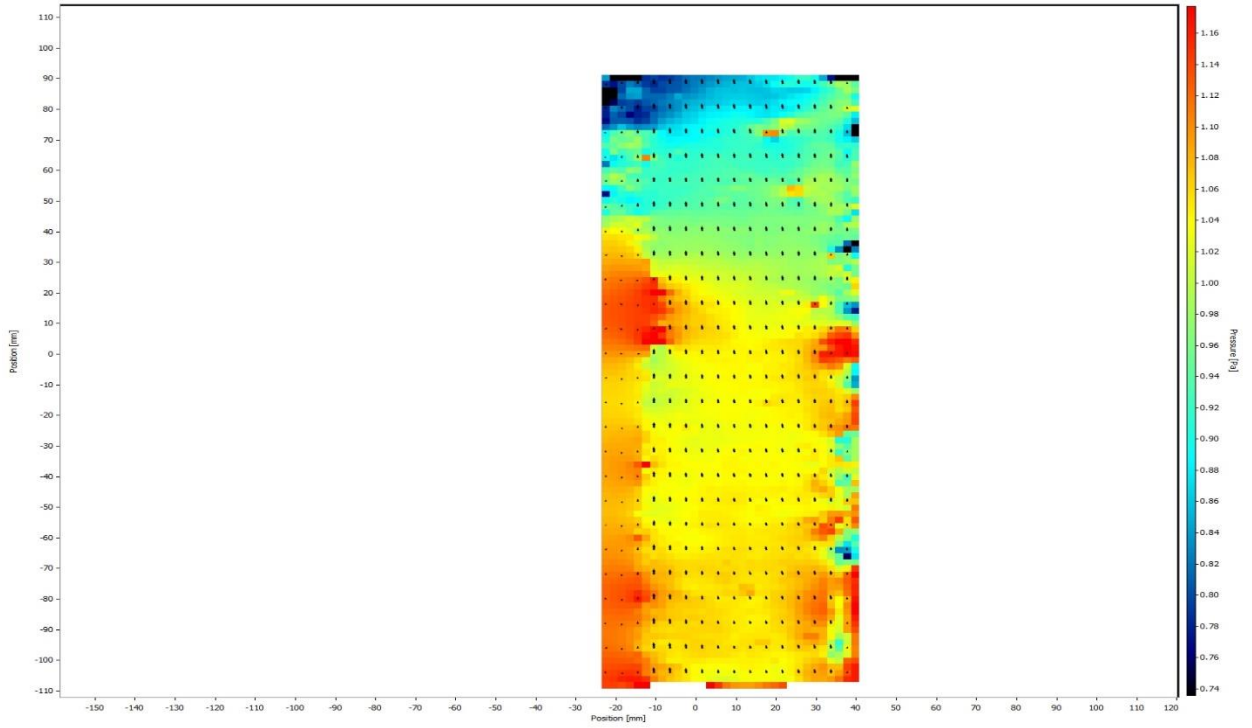

Pressure at 1.45 m/s

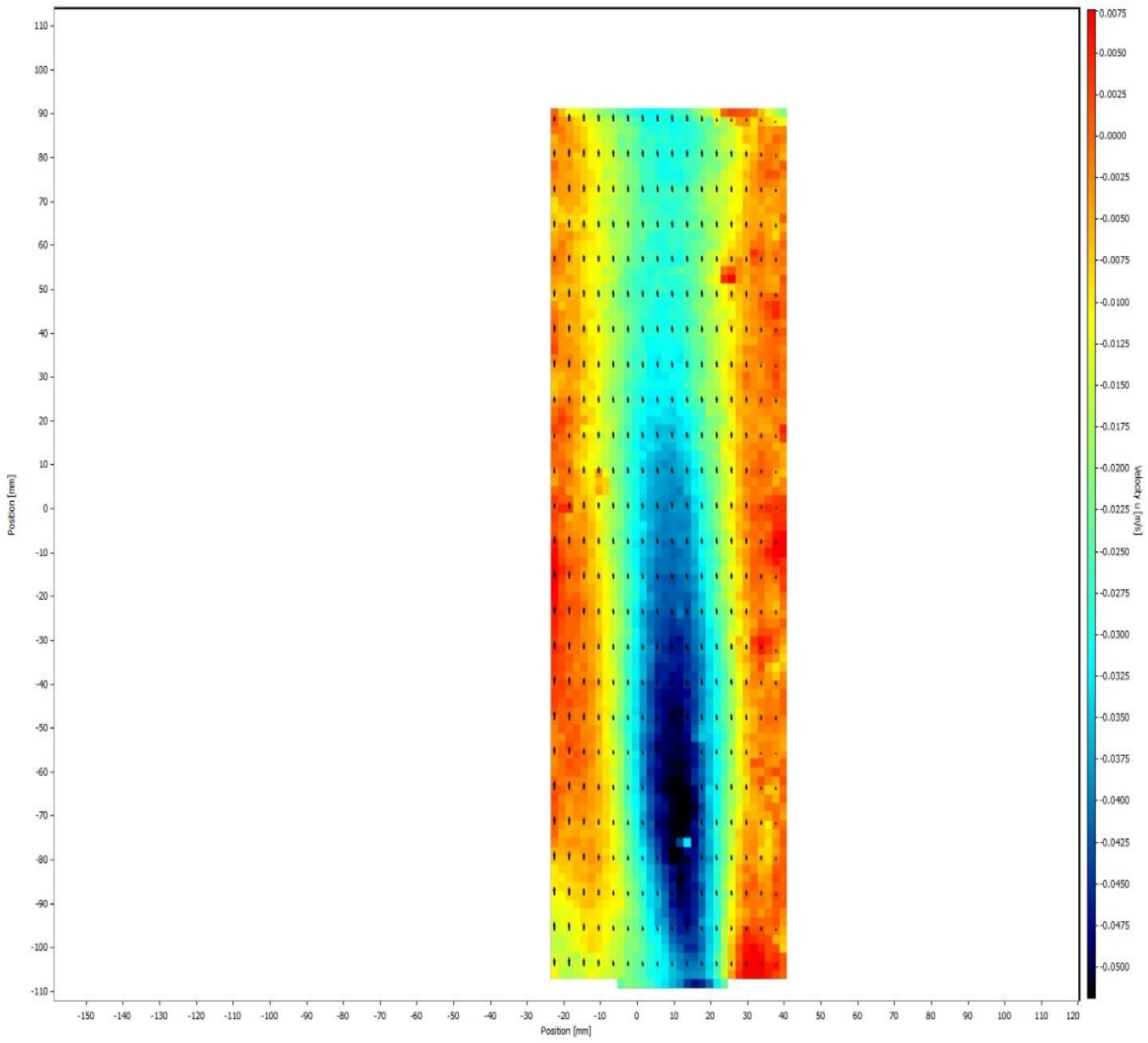

Velocity at 0.0021 m^3/s

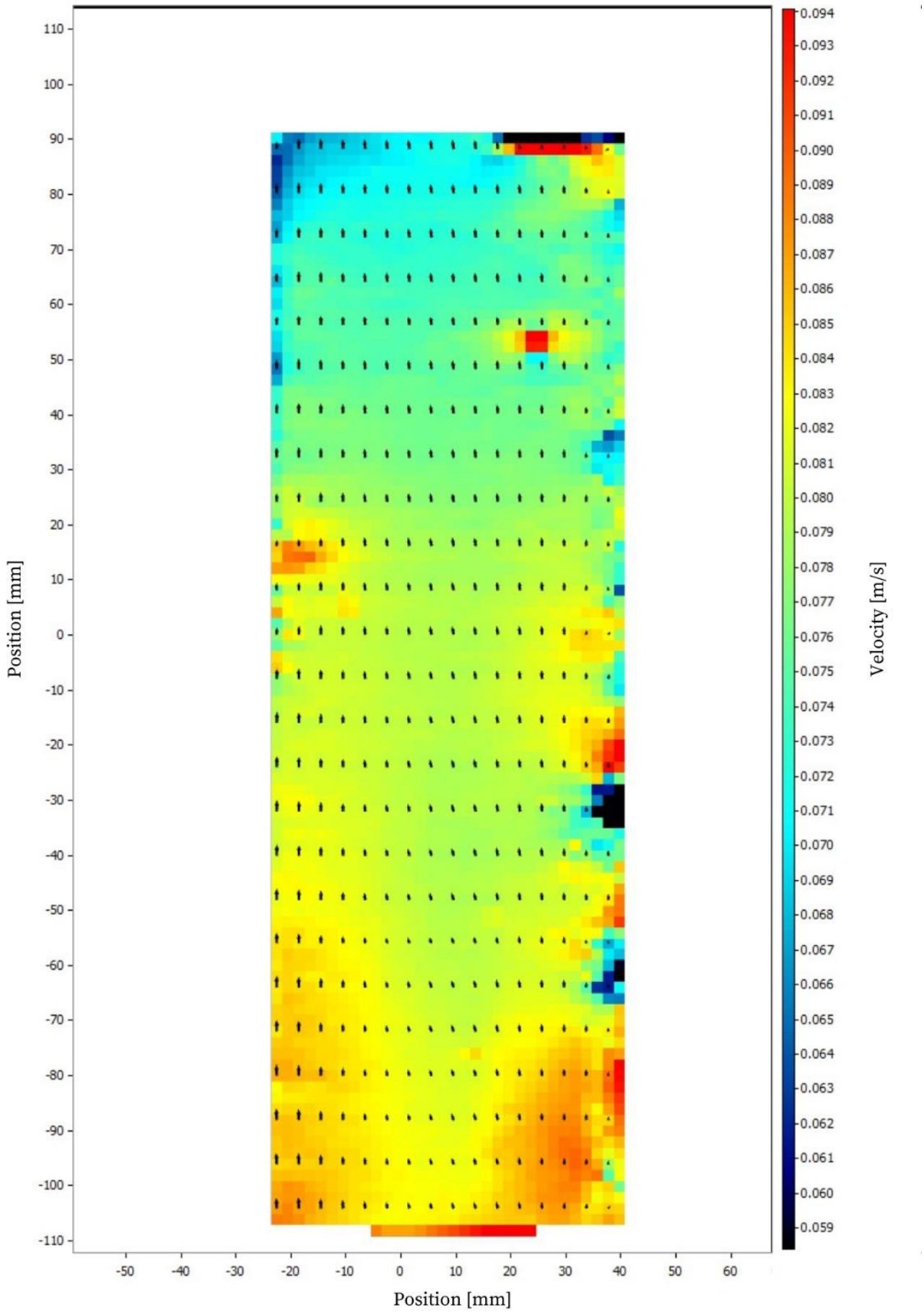

Pressure at 0.42 m/s

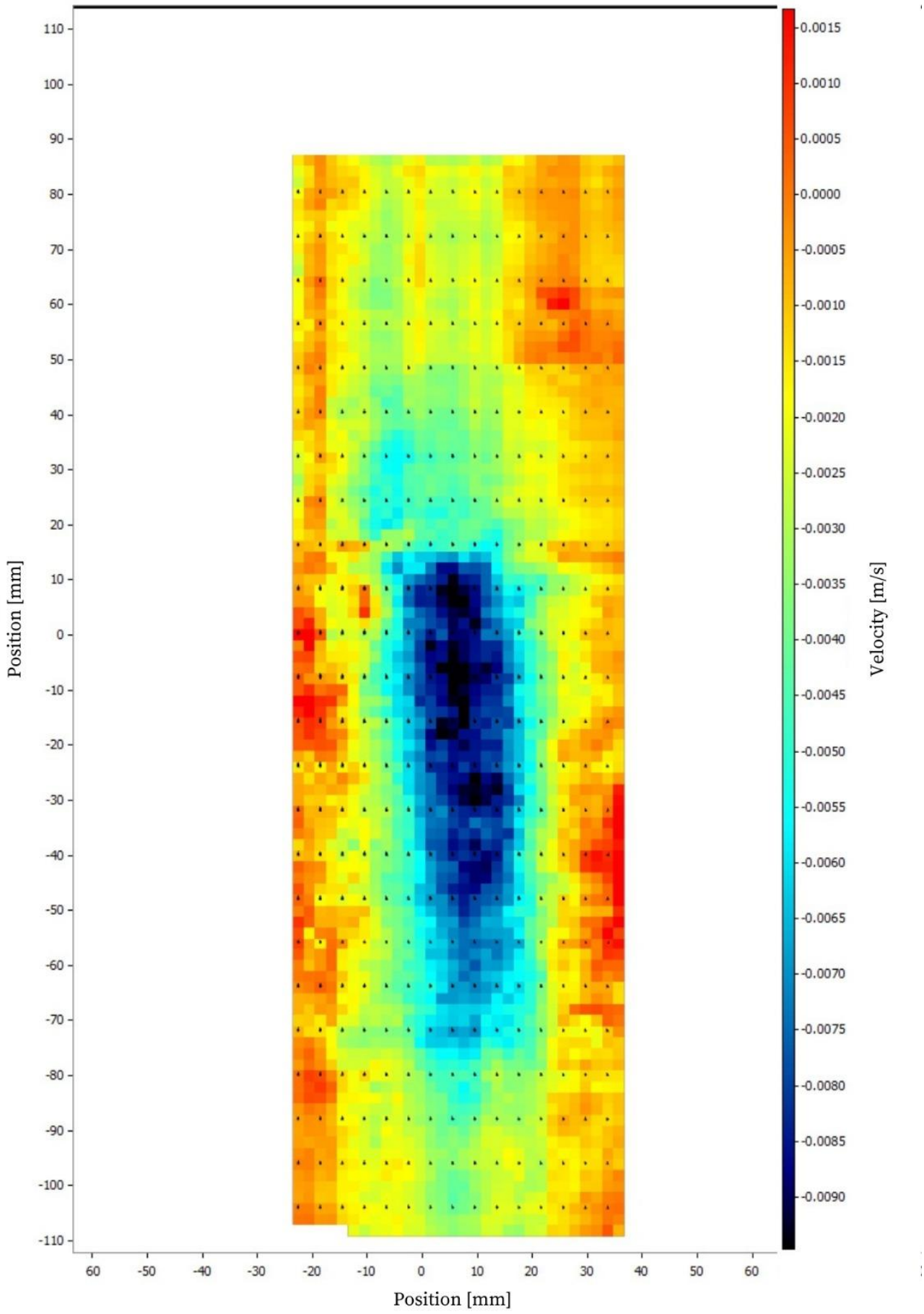

Velocity at 0.001 m^3/s

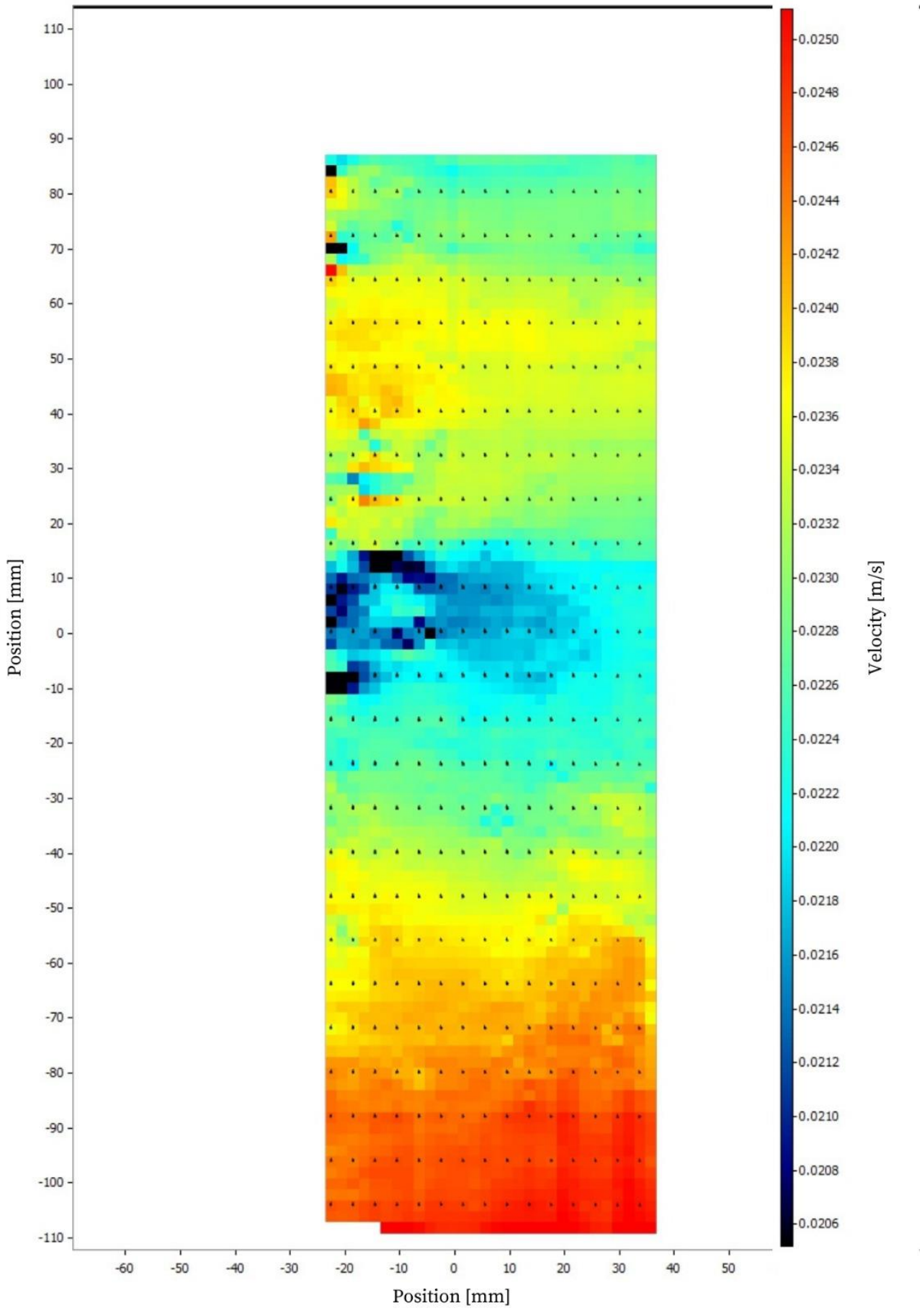

Pressure field for 0.2 m/s